Supporting information

Host Metabolic Response in Early Lyme Disease

Bryna L. Fitzgerald[1], Claudia R. Molins[1], M. Nurul Islam[2], Barbara Graham[2], Petronella R. Hove Magunda[2], Gary Wormser[3], Linden Hu[4], Laura V. Ashton[1], and John T. Belisle[2]*.

[1]Centers for Disease Control and Prevention, Fort Collins, CO 80521, USA.

[2]Deparment of Microbiology, Immunology, and Pathology, Colorado State University, Fort Collins, CO 80521, USA.

[3]Division of Infectious Diseases, Department of Medicine, New York Medical College,Valhalla, NY 10595, USA.

[4]Sackler School of Graduate Biomedical Sciences, Tufts University School of Medicine, Boston, Massachusetts 02111, USA.

***Corresponding author:** John T. Belisle: john.belisle@colostate.edu (Tel: 970-491-5384)

Table of Contents

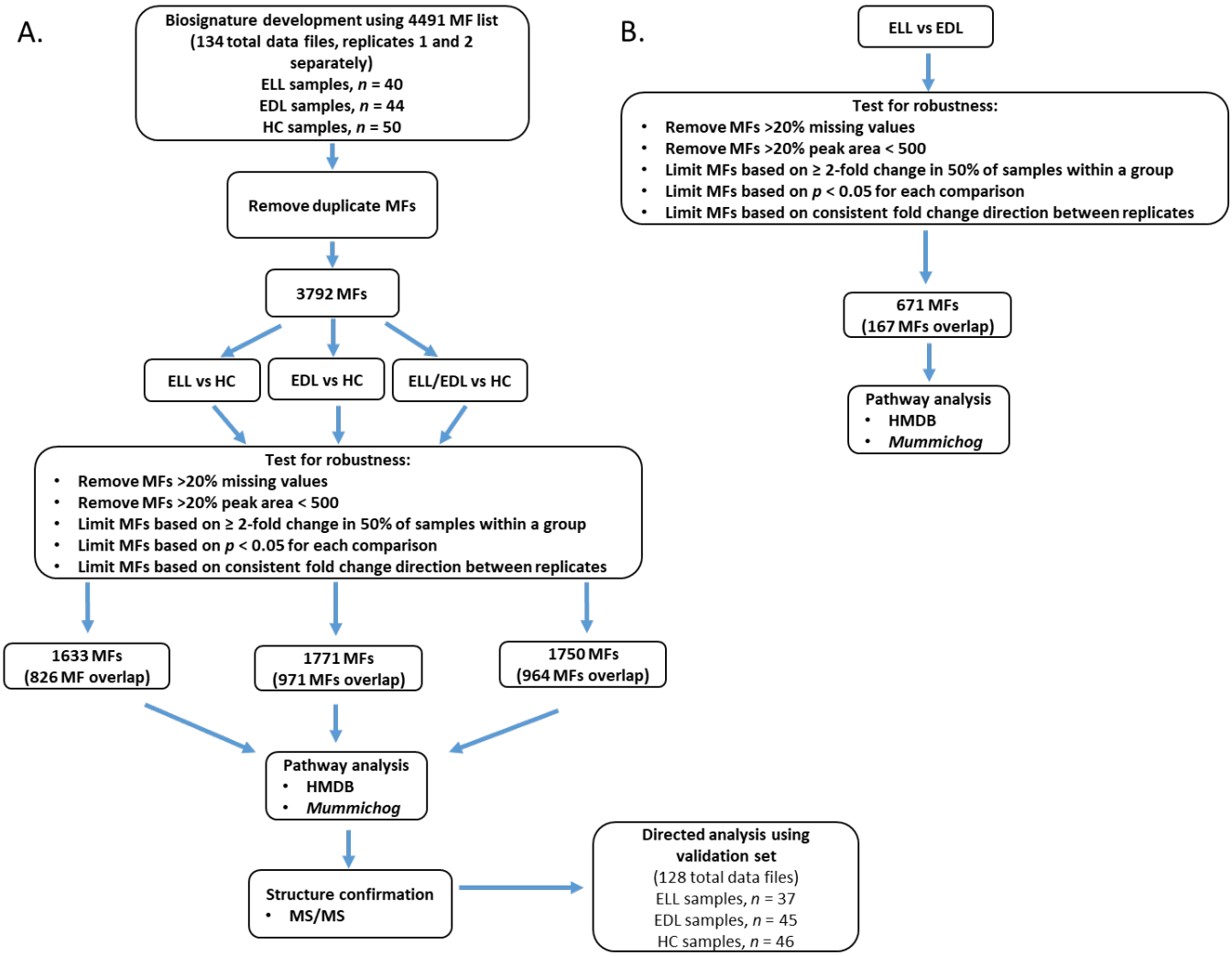

Figure S-1. Workflow utilized for biosignature development, pathway analyses and validation. For the early Lyme disease vs HC biosignature (A). Two replicate LC-MS analyses of early Lyme disease (ELL and EDL) samples and HC were combined to identify a list of differentiating MFs for four comparisons (ELL vs HC, EDL vs HC, ELL/EDL vs HC, and ELL vs EDL). The data from both LC-MS replicates were combined and screened for consistency and robustness which resulted in four biosignatures: 1633 MFs for ELL vs HC, 1771 MFs for EDL vs HC, 1750 for ELL/EDL vs HC. These biosignatures were used for downstream pathway analyses and directed analysis in a separate validation set of early Lyme disease and HC samples. An identical process was used for generation and analysis of the ELL vs EDL biosignature consisting of 671 MFs (B).

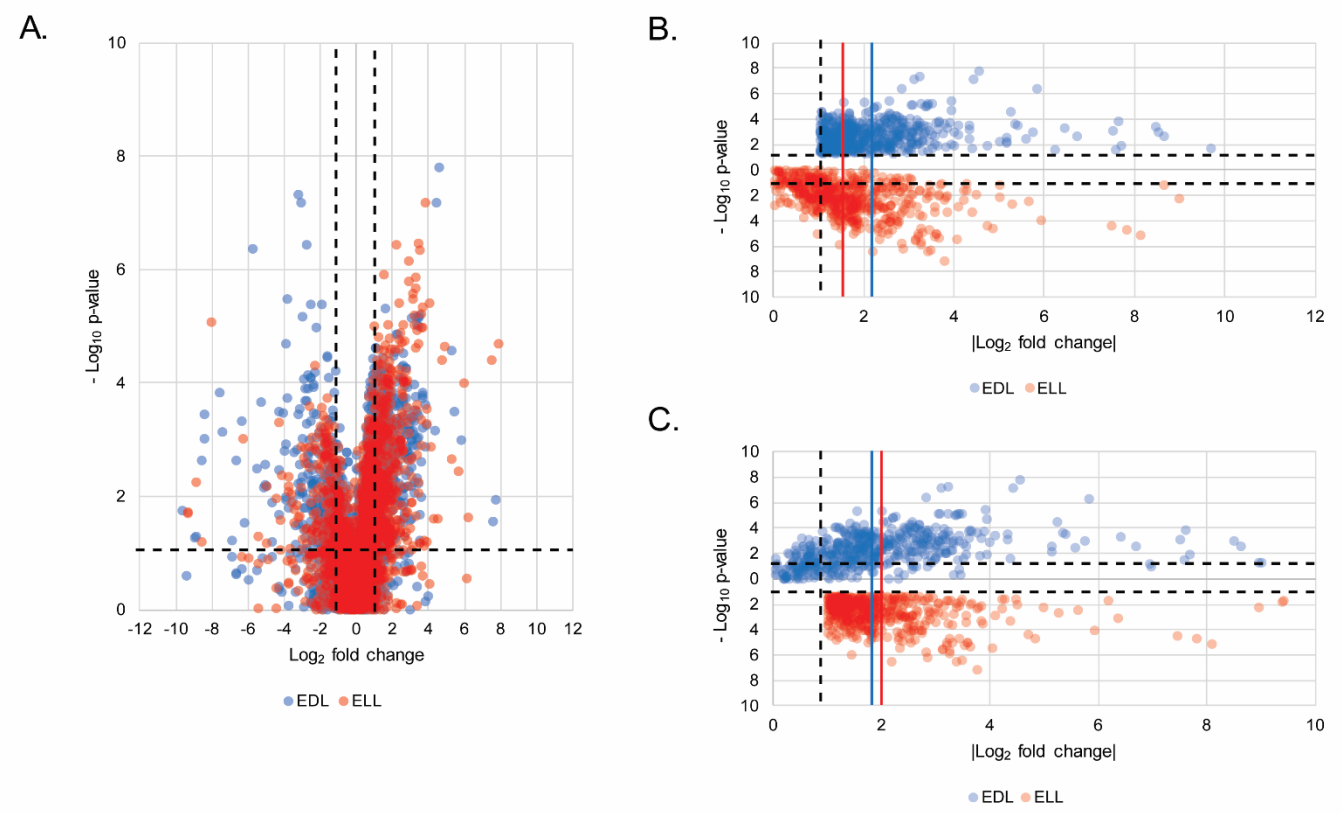

Figure S-2. Volcano plot depicting the $\log_2$ fold change (x-axis) and $-\log_{10}$ p-value (y-axis) for the 2193 MFs (from the combined early Lyme disease vs HC biosignature) as compared to HC. MFs in EDL and ELL are plotted in blue and red, respectively, for replicate 2. The upper left quadrant contains 247 and 178 MFs and the upper right quadrant contains 374 and 379 MFs for EDL and ELL, respectively (A). A plot of $|\log_2$ fold change from HC$|$ (x-axis) and $-\log_{10}$ p-value (y-axis) for the 621 MFs with >1 $\log_2$ fold change and $p < 0.05$ in the EDL vs HC comparison plotted for EDL (blue) and ELL (red) for replicate 2 (B). A plot of $\log_2$ fold change from HC (x-axis) and $-\text{Log}_{10}$ p-value (y-axis) for the 557 MFs with > 1 $\log_2$ fold change and $p < 0.05$ in the ELL vs HC comparison plotted for EDL (blue) and ELL (red) for replicate 2 (C). The vertical blue lines depict the approximate mean fold change (2.13 +/- 1.16 and 1.90 +/- 1.36 for B and C respectively) for EDL vs HC and the vertical red lines depict the approximate mean fold change (1.65 +/- 1.15 and 1.96 +/- 1.09 for B and C respectively) for ELL vs HC.

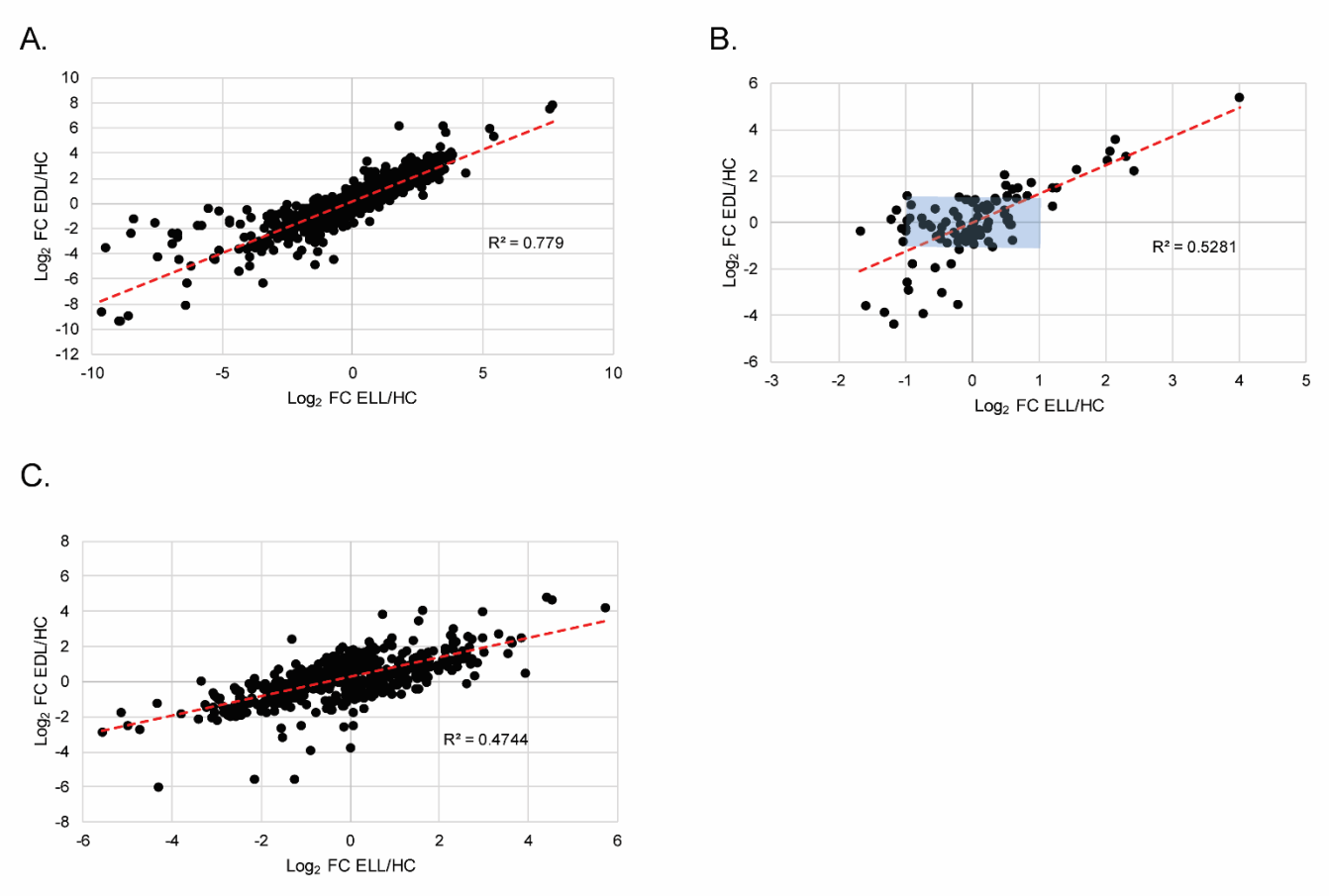

Figure S-3. Scatter plots for replicate 2 depicting $\log_2$ fold change from HC for EDL (x-axis) and $\log_2$ fold change from HC for ELL (y-axis) using the 1627 MFs unique to the EL vs HC biosignature (A); or the 105 MFs unique to the ELL vs EDL biosignature (B); or the 566 MFs in common between the early Lyme disease vs HC and the ELL vs EDL biosignatures (C). The red dotted line is the line of best fit. Blue shaded box indicates 71 out of 105 MFs with a $|\log_2$ fold change$| \leq 1$ from HC for EDL and ELL.

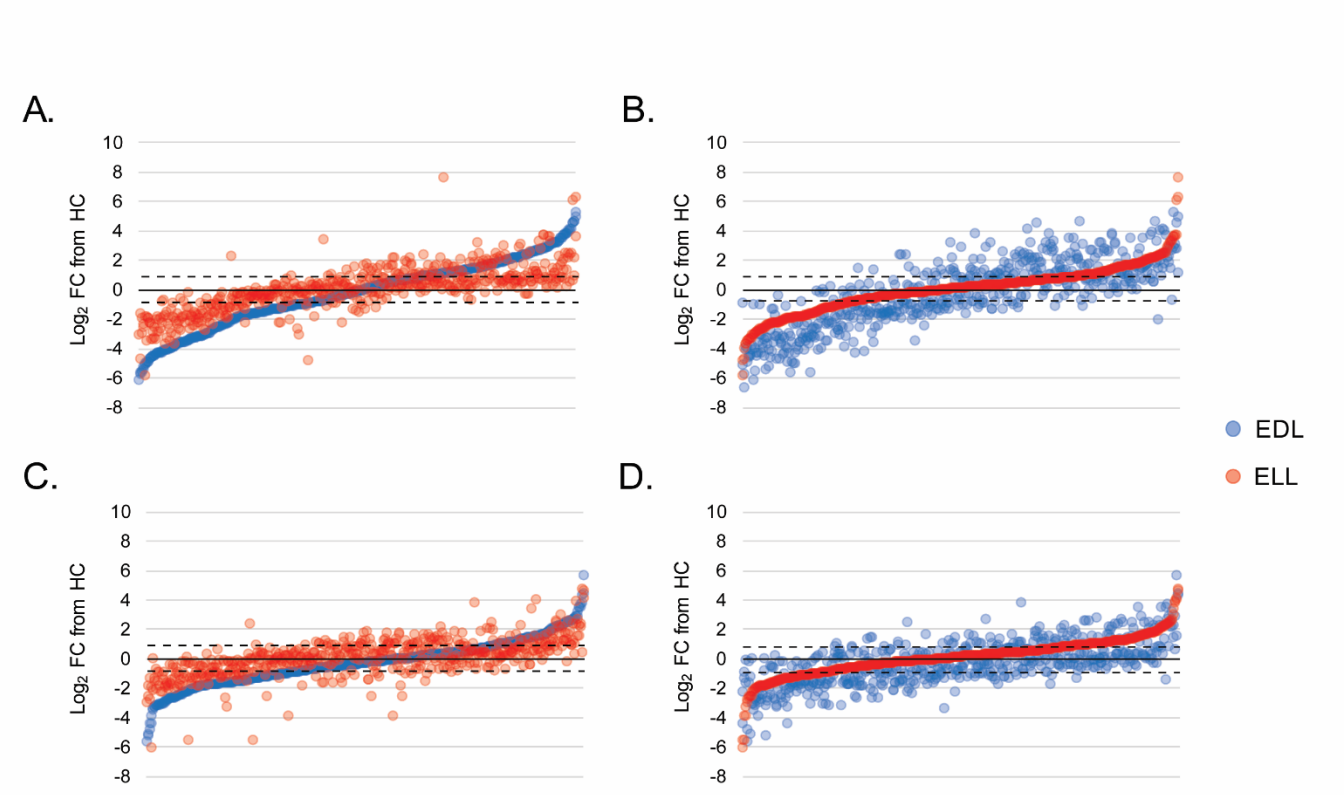

Figure S-4. Scatter plots depicting the $\log_2$ fold change from HC for the 566 MFs in common between the early Lyme disease vs HC and the ELL vs EDL biosignatures. The MFs of the ELL and EDL patients are plotted in red and blue, respectively. The scatter plots are organized by replicate 1 (A and B) and replicate 2 (C and D) and depict the fold change magnitude for ELL (B and D) and EDL (A and C) . Solid lines and dotted lines represent 0 and +/- 1 $\log_2$ fold change from HC, respectively.

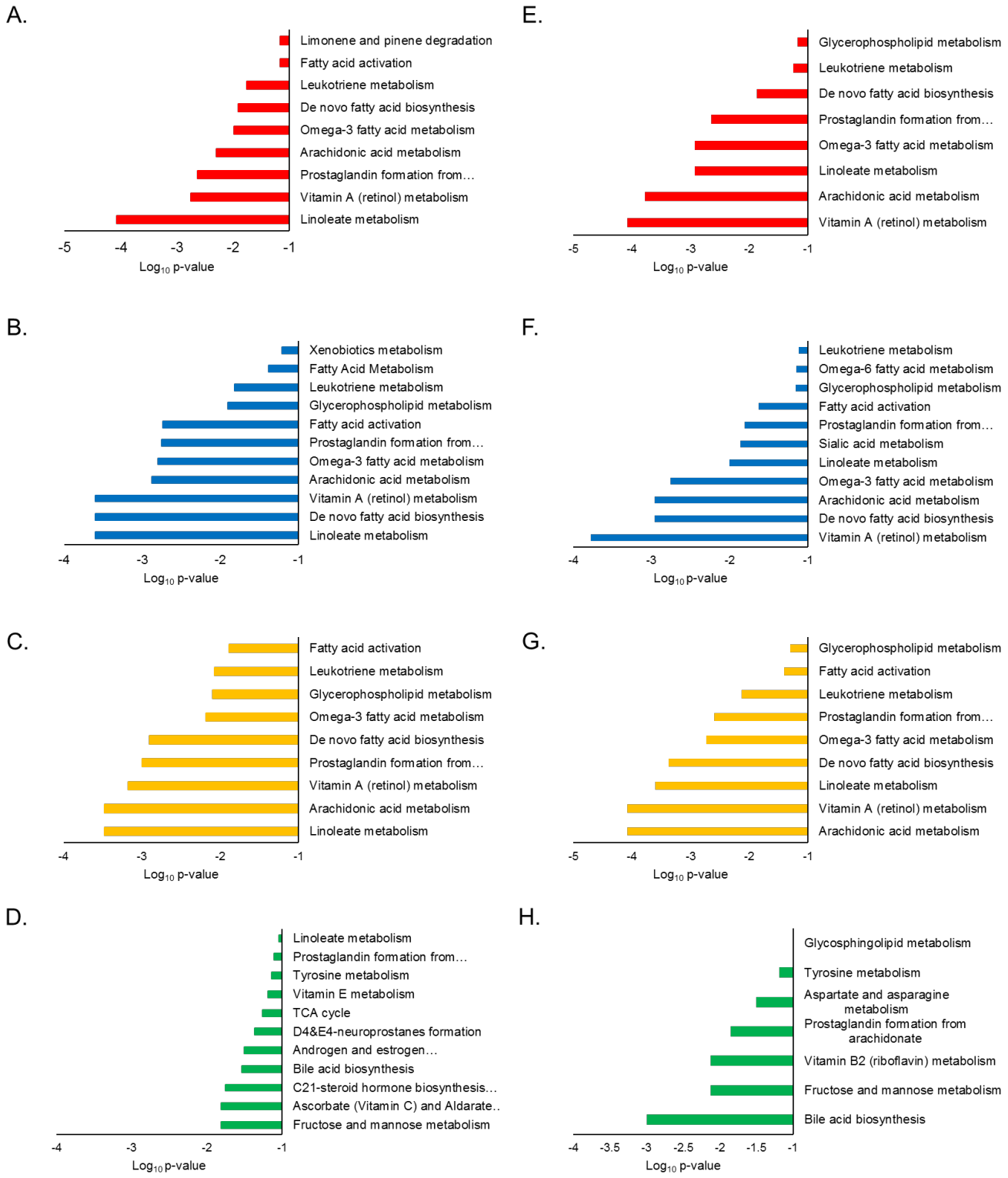

Figure S-5. *Mummichog* enriched pathways and level of enrichment (log_{10} p-value) for replicate 1 (A-D) and replicate 2 (E-H) for ELL vs HC (A and E), EDL vs HC (B and F), ELL/EDL vs HC (C and G), and ELL vs EDL (D and H) biosignatures.

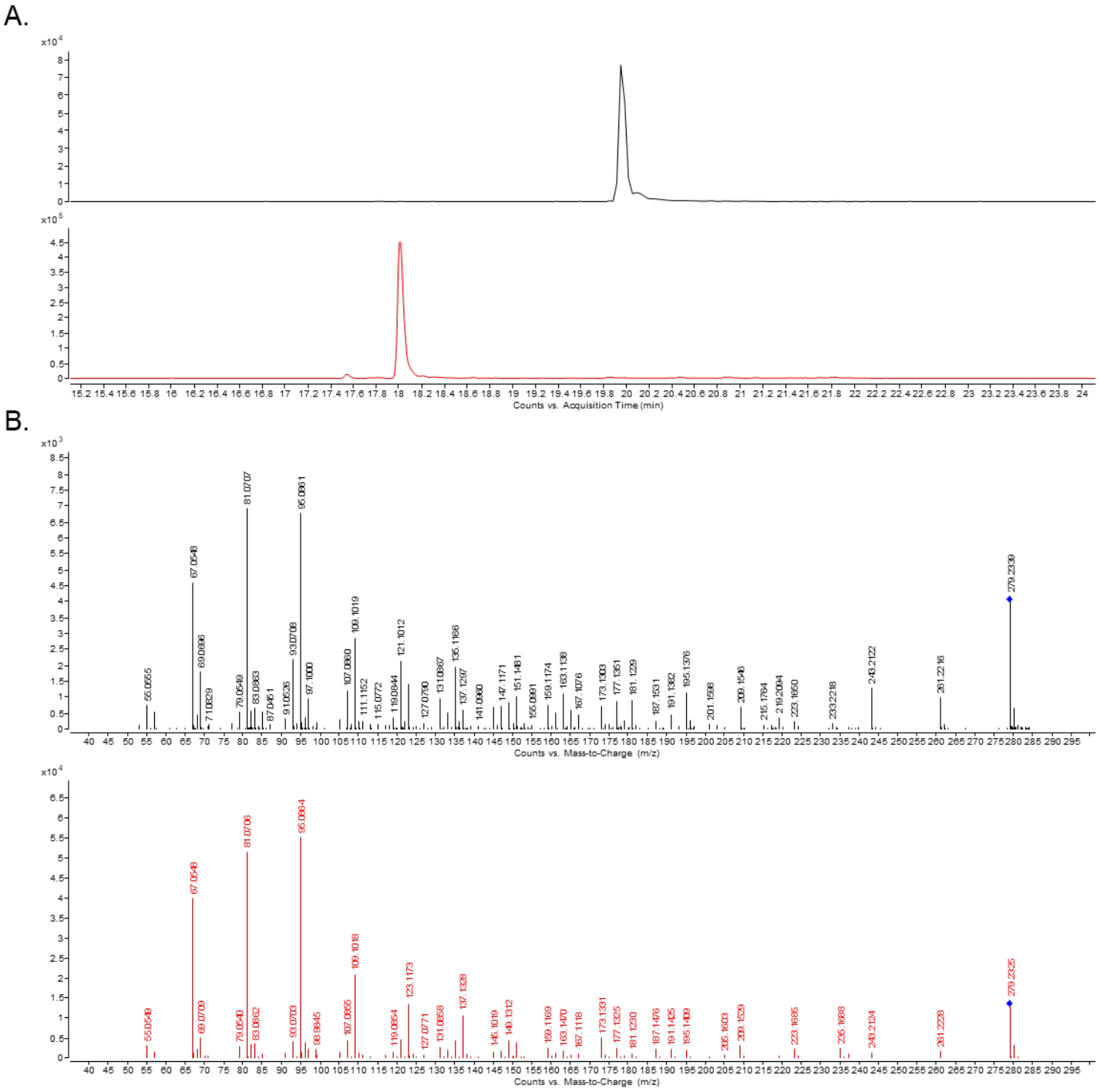

Figure S-6. LC-MS/MS confirmation MF# 1823 as a polyunsaturated fatty acid metabolite. Extracted ion chromatogram (EIC) for *m/z* 279.2327 (positive mode ionization) demonstrates a different retention time (RT) in a pooled patient sample than that for γ-linolenic acid standard (A). MS/MS fragmentation for MF# 1823 and γ-linolenic acid resulted in common MS/MS fragmentation patterns (B). Chromatograms and spectra corresponding to the pooled patient sample are depicted in red and those corresponding to the standard are depicted in black.

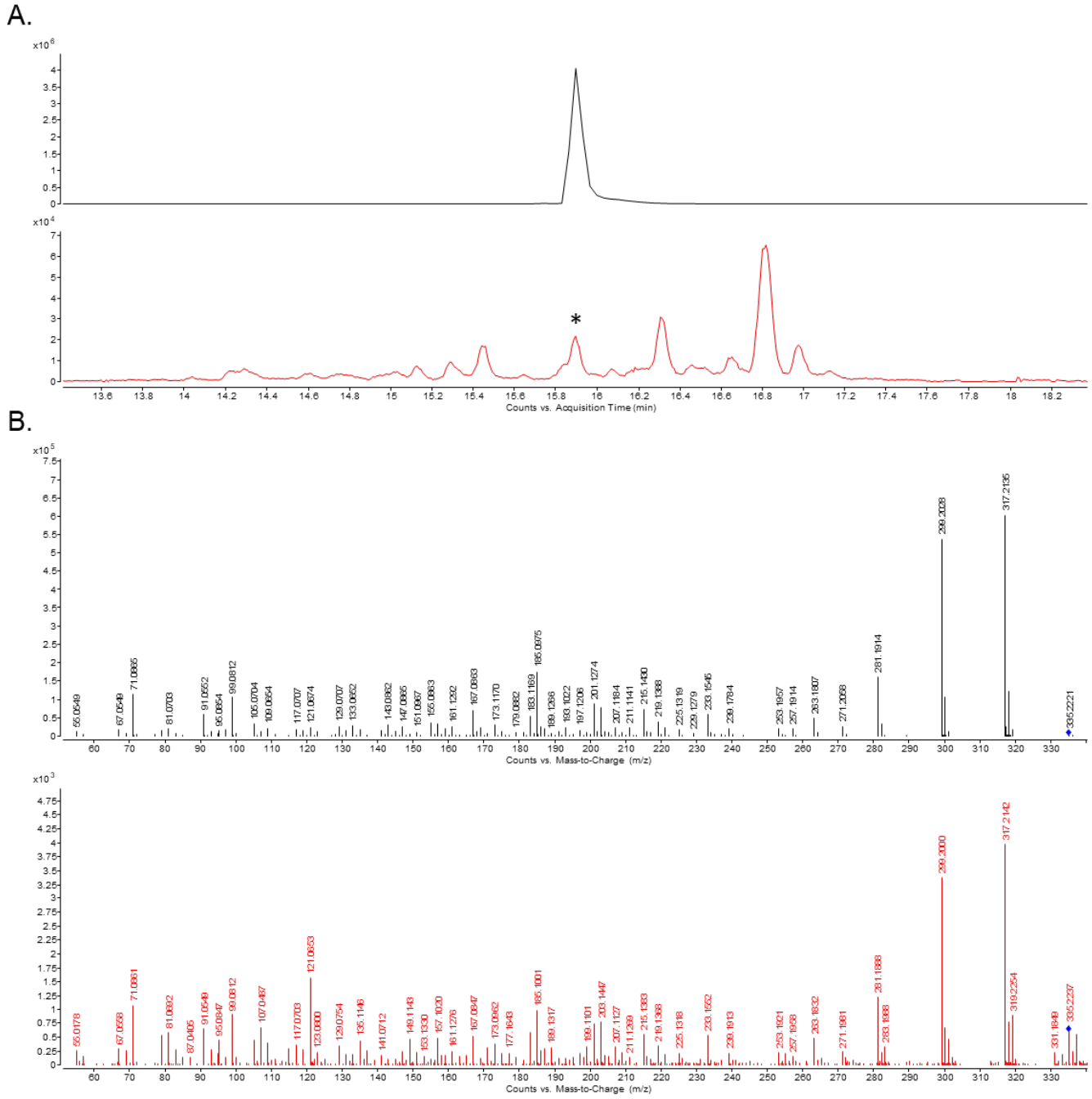

Figure S-7. LC-MS/MS confirmation MF# 2298 as prostaglandin B2. Extracted ion chromatogram (EIC) for *m/z* 335.2208 (positive mode ionization) demonstrates matching RT in a pooled patient sample and that for prostaglandin B2 standard (A). MS/MS fragmentation for MF# 2298 and prostaglandin B2 resulted in common MS/MS fragmentation patterns (B). Chromatograms and spectra corresponding to the pooled patient sample are depicted in red and those corresponding to the standard are depicted in black. Star indicates the MF peak of interest.

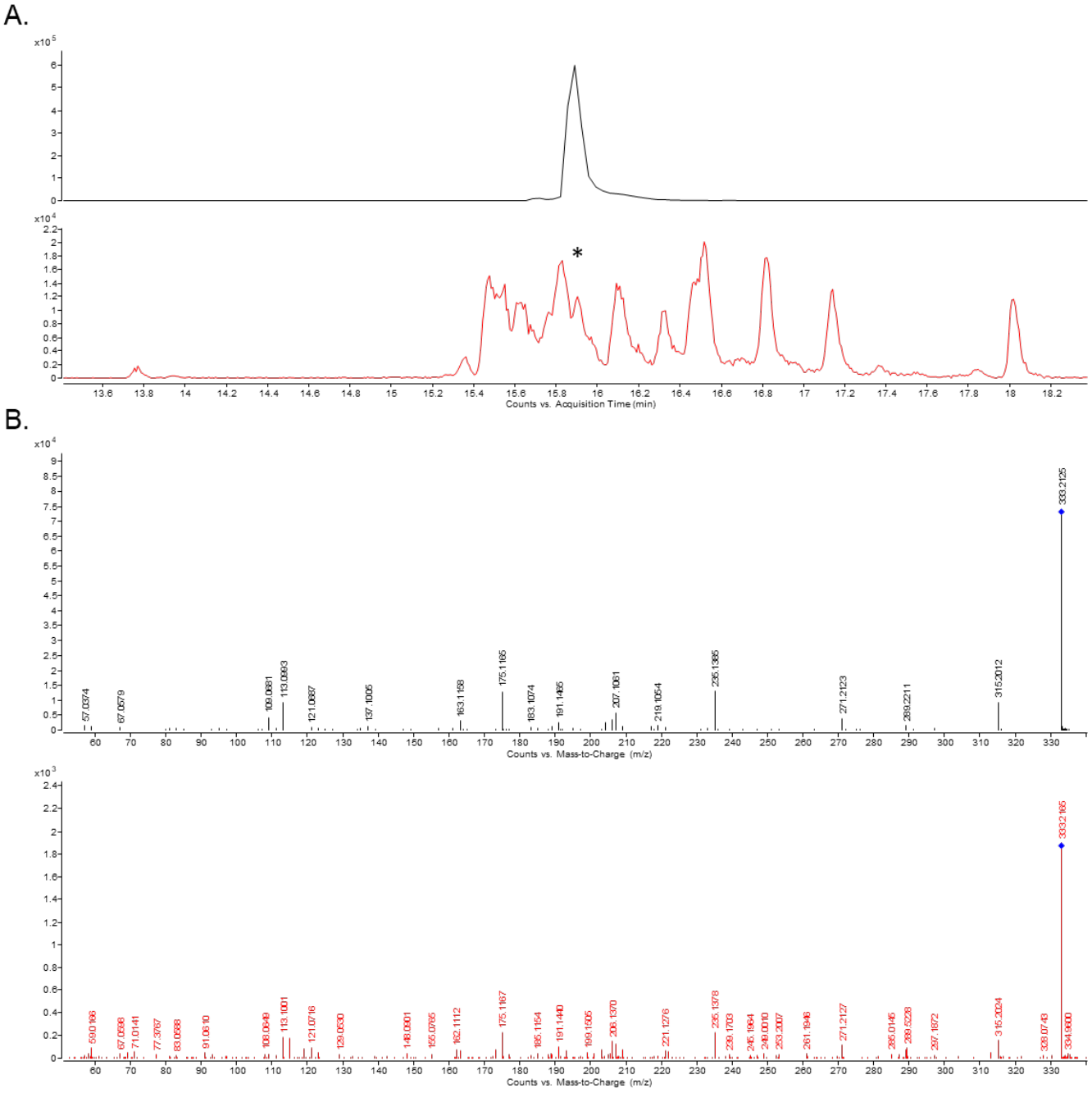

Figure S-8. LC-MS/MS confirmation of MF# 2298 as prostaglandin B2. Extracted ion chromatogram (EIC) for *m/z* 333.2071 (negative mode ionization) demonstrates matching RT in a pooled patient sample and that for prostaglandin B2 standard (A). MS/MS fragmentation for MF# 2298 and prostaglandin B2 resulted in common MS/MS fragmentation patterns (B). Chromatograms and spectra corresponding to the pooled patient sample are depicted in red and those corresponding to the standard are depicted in black. Star indicates the MF peak of interest.

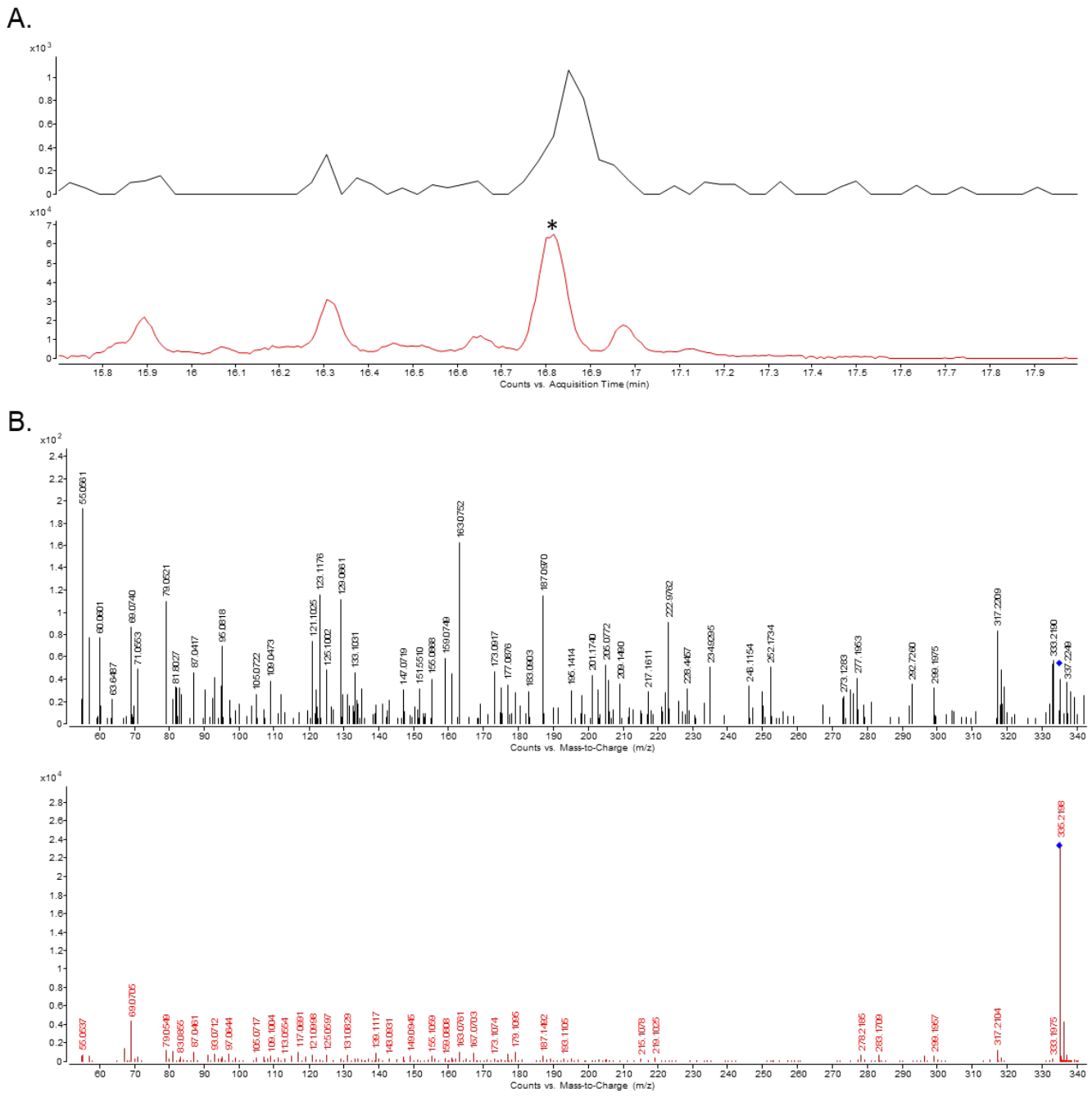

Figure S-9. LC-MS/MS confirmation of MF# 1241 as 12-oxo-leukotriene B4. Extracted ion chromatogram (EIC) for *m/z* 335.2208 (positive mode ionization) demonstrates matching RT in a pooled patient sample and that for 12-oxo-leukotriene B4 standard (A). MS/MS fragmentation for MF# 1241 and 12-oxo-leukotriene B4 resulted in common MS/MS fragmentation patterns (B). Chromatograms and spectra corresponding to the pooled patient sample are depicted in red and those corresponding to the standard are depicted in black. Star indicates the MF peak of interest.

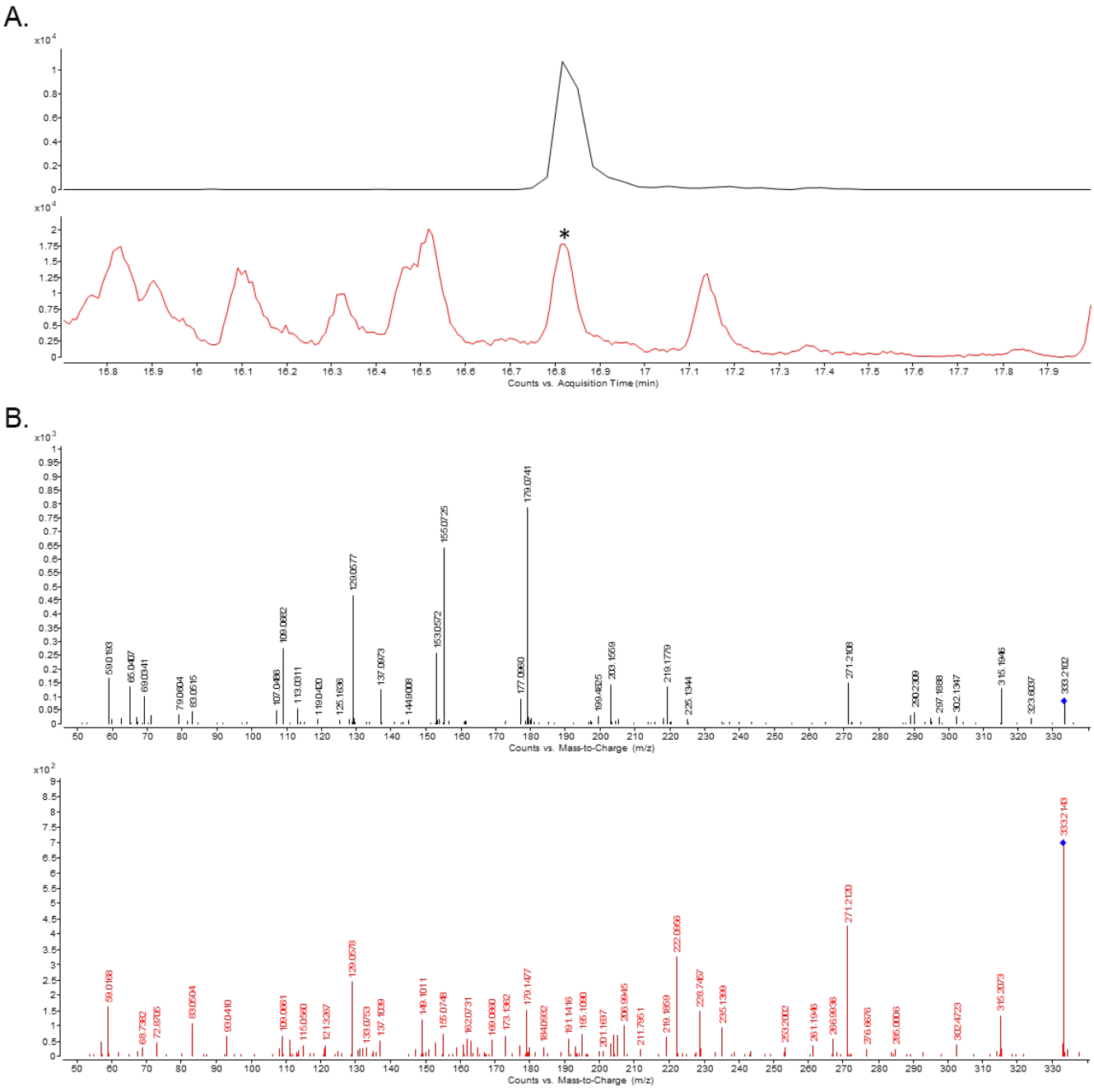

Figure S-10. LC-MS/MS confirmation of MF# 1241 as 12-oxo-leukotriene B4. Extracted ion chromatogram (EIC) for *m/z* 333.2071 (negative mode ionization) demonstrates matching RT in a pooled patient sample and that for 12-oxo-leukotriene B4 standard (A). MS/MS fragmentation for MF# 1241 and 12-oxo-leukotriene B4 resulted in common MS/MS fragmentation patterns (B). Chromatograms and spectra corresponding to the pooled patient sample are depicted in red and those corresponding to the standard are depicted in black. Star indicates the MF peak of interest.

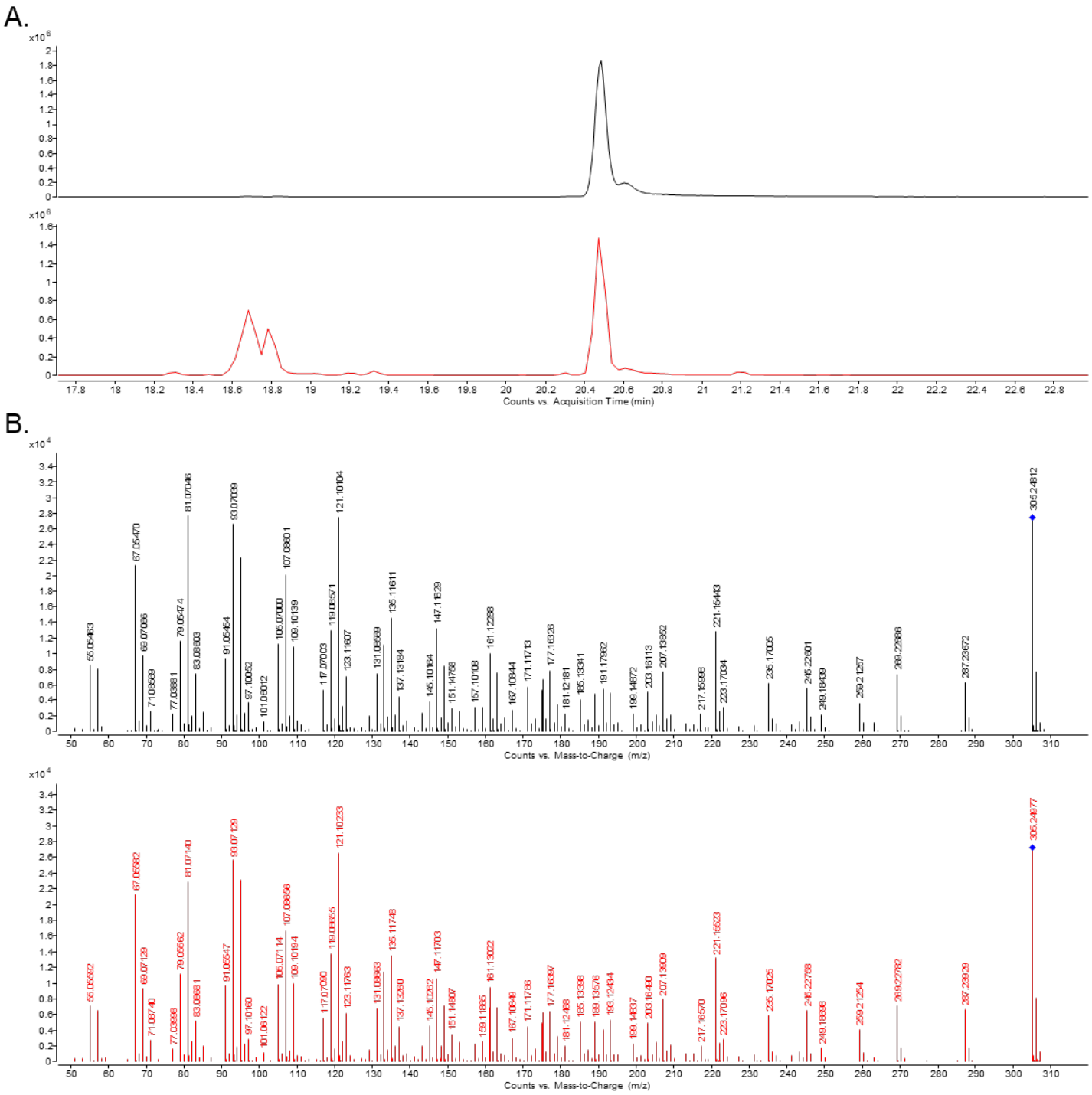

Figure S-11. LC-MS/MS confirmation of MF# 1269 as arachidonic acid. Extracted ion chromatogram (EIC) for *m/z* 305.2475 (positive mode ionization) demonstrates matching RT in a pooled patient sample and that for arachidonic acid standard (A). MS/MS fragmentation for MF# 1269 and arachidonic acid resulted in common MS/MS fragmentation patterns (B). Chromatograms and spectra corresponding to the pooled patient sample are depicted in red and those corresponding to the standard are depicted in black.

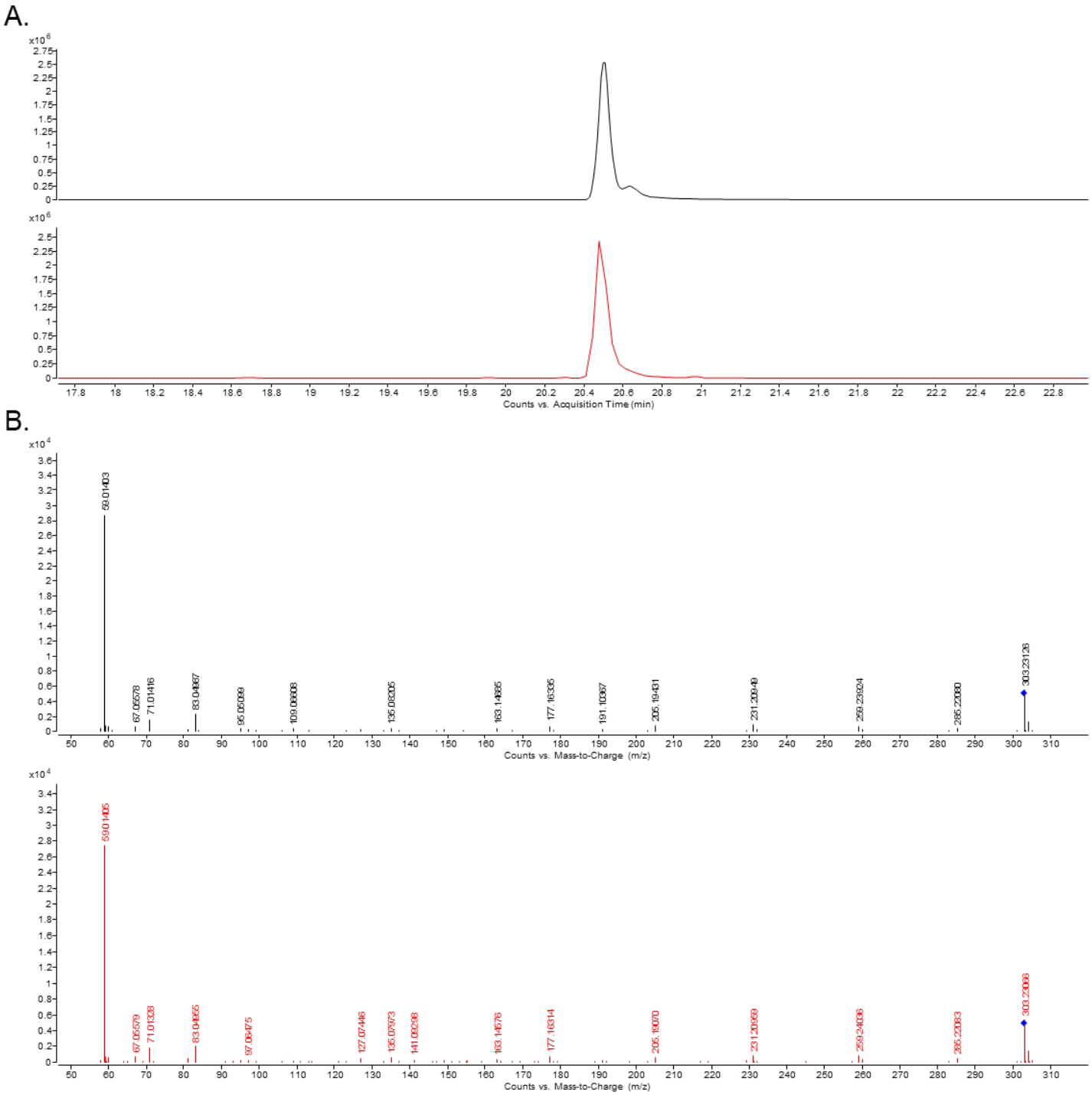

Figure S-12. LC-MS/MS confirmation of MF# 1269 as arachidonic acid. Extracted ion chromatogram (EIC) for *m/z* 303.2330 demonstrates matching RT in a pooled patient sample and that for arachidonic acid standard (A). MS/MS fragmentation for MF# 1269 and arachidonic acid resulted in common MS/MS fragmentation patterns (B). Chromatograms and spectra corresponding to the pooled patient sample are depicted in red and those corresponding to the standard are depicted in black.

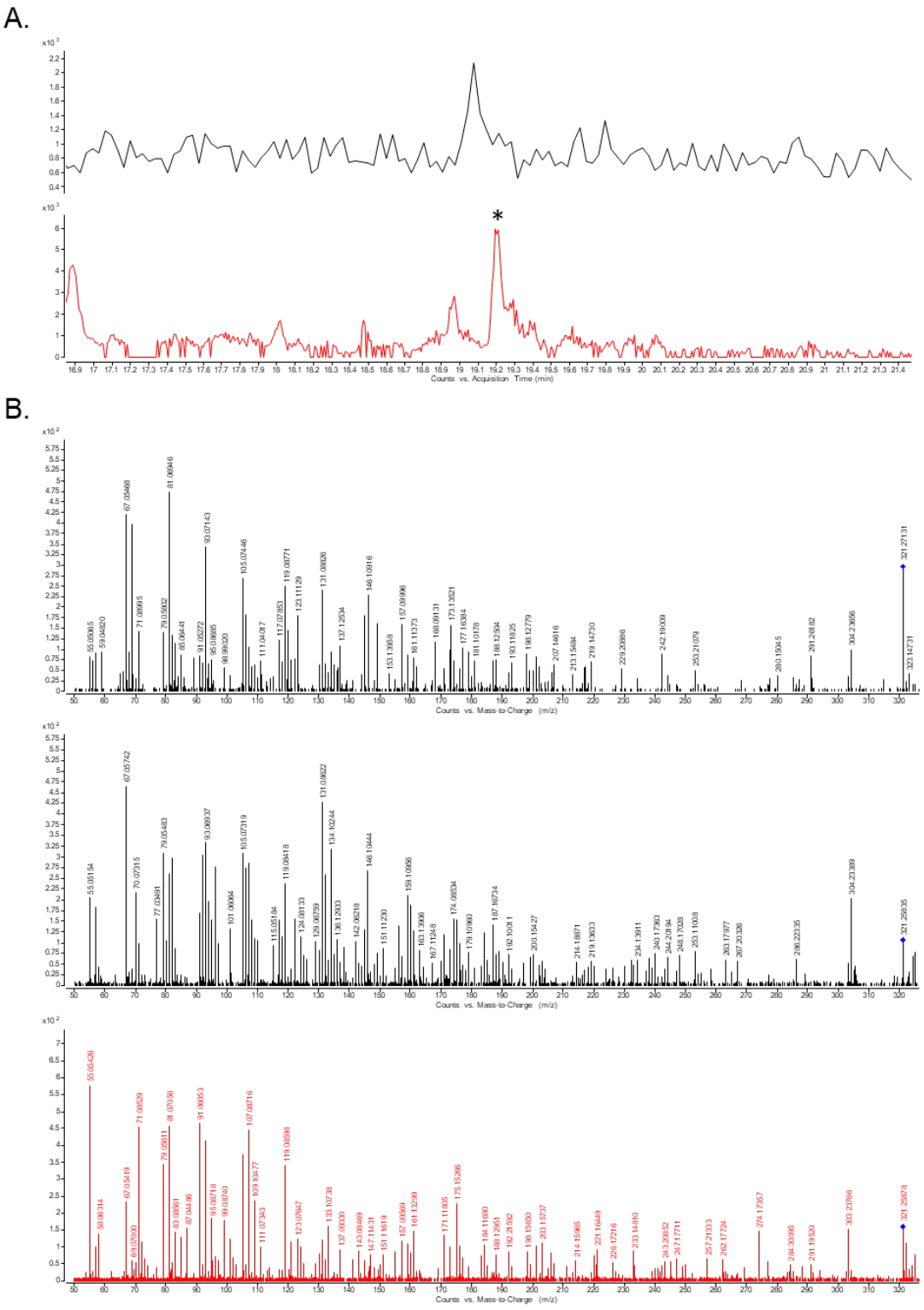

Figure S-13. LC-MS/MS confirmation of MF# 1841 as hydroxyeicosatetraenoic acid (HETE). Extracted ion chromatogram (EIC) for *m/z* 321.2424 (positive mode ionization) demonstrates matching RT in a pooled patient sample and that for 12R-hydroxyeicosatetraenoic acid standard (A). MS/MS fragmentation for MF# 1841 and 12R-hydroxyeicosatetraenoic acid (top) and 8S-hydroxyeicosatetraenoic acid (middle) resulted in common MS/MS fragmentation patterns (B). Chromatograms and spectra corresponding to the pooled patient sample are depicted in red and those corresponding to the standard are depicted in black. Star indicates the MF peak of interest.

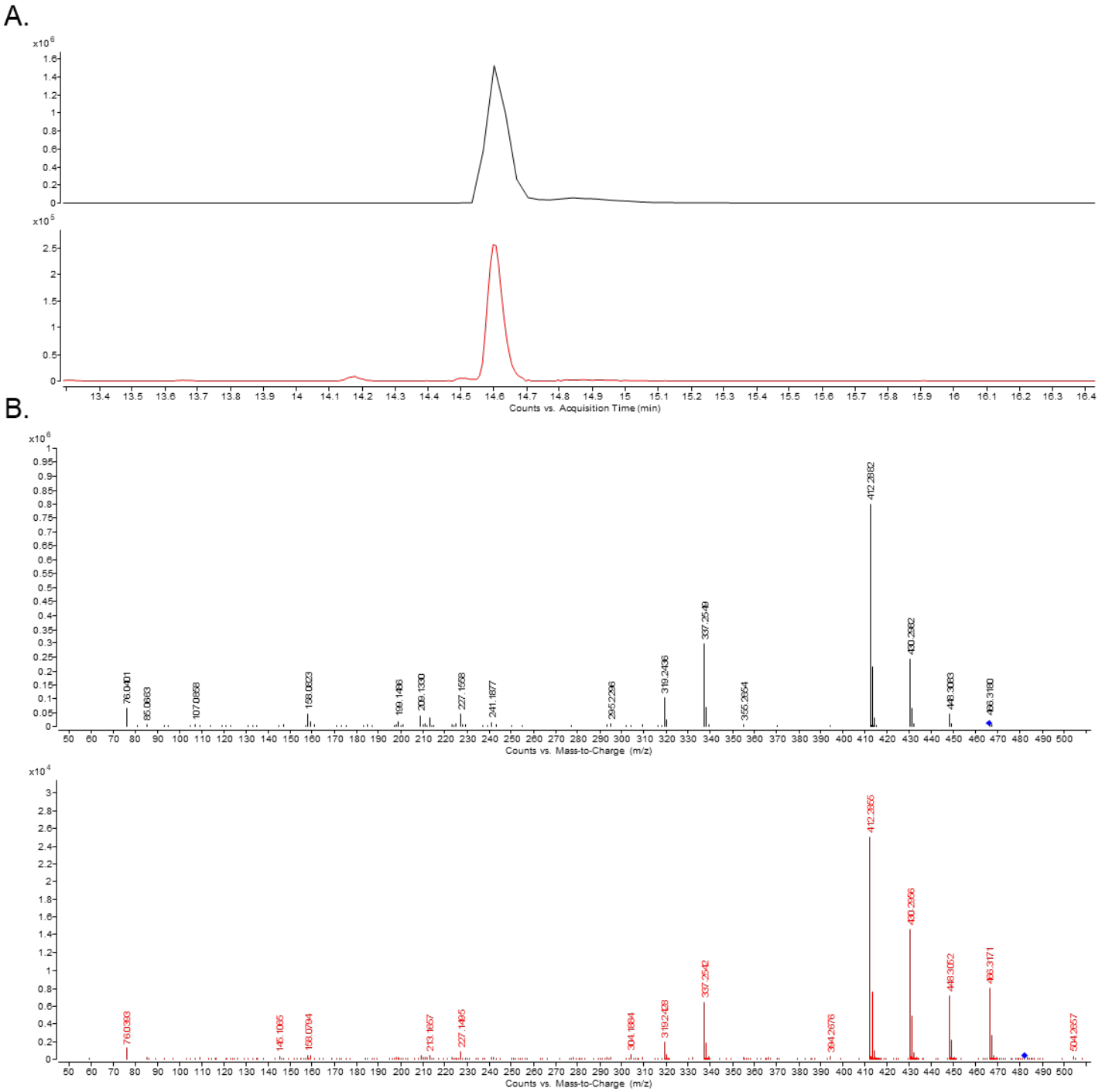

Figure S-14. LC-MS/MS confirmation of MF# 53 as glycocholic acid. Extracted ion chromatogram (EIC) for *m/z* 466.3220 (positive mode ionization) demonstrates matching RT in a pooled patient sample and that for glycocholic acid standard (A). MS/MS fragmentation for MF# 53 and glycocholic acid resulted in common MS/MS fragmentation patterns (B). Chromatograms and spectra corresponding to the pooled patient sample are depicted in red and those corresponding to the standard are depicted in black.

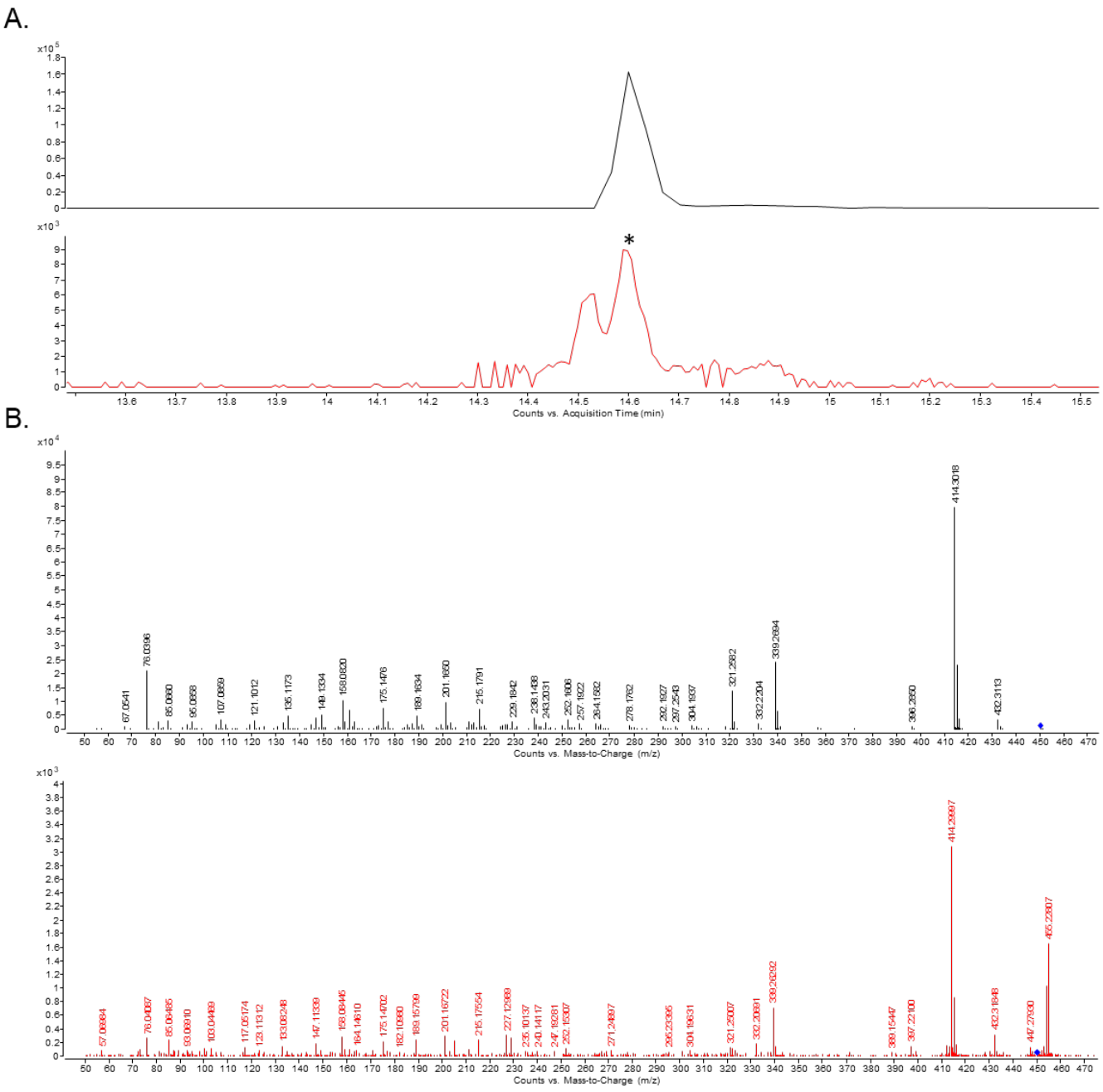

Figure S-15. LC-MS/MS confirmation of MF# 1601 as glycoursodeoxycholic acid. Extracted ion chromatogram (EIC) for *m/z* 450.3209 (positive mode ionization) demonstrates matching RT in a pooled patient sample and that for glycoursodeoxycholic acid standard (A). MS/MS fragmentation for MF# 1601 and glycoursodeoxycholic acid resulted in common MS/MS fragmentation patterns (B). Chromatograms and spectra corresponding to the pooled patient sample are depicted in red and those corresponding to the standard are depicted in black. Star indicates the MF peak of interest.

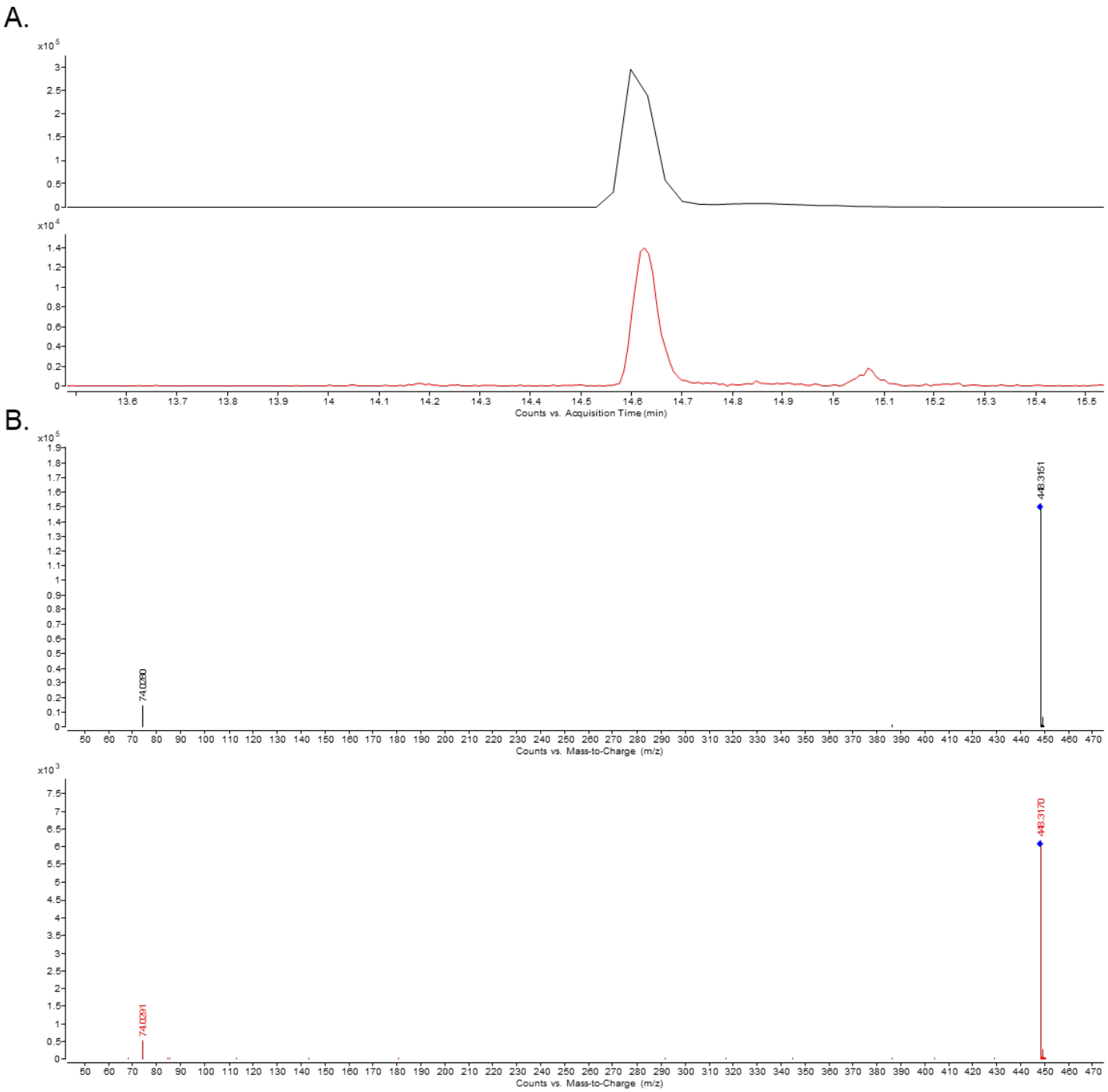

Figure S-16. LC-MS/MS confirmation of MF# 1601 as glycoursodeoxycholic acid. Extracted ion chromatogram (EIC) for *m/z* 448.3068 (negative mode ionization) demonstrates matching RT in a pooled patient sample and that for glycoursodeoxycholic acid standard (A). MS/MS fragmentation for MF# 1601 and glycoursodeoxycholic acid resulted in common MS/MS fragmentation patterns (B). Chromatograms and spectra corresponding to the pooled patient sample are depicted in red and those corresponding to the standard are depicted in black.

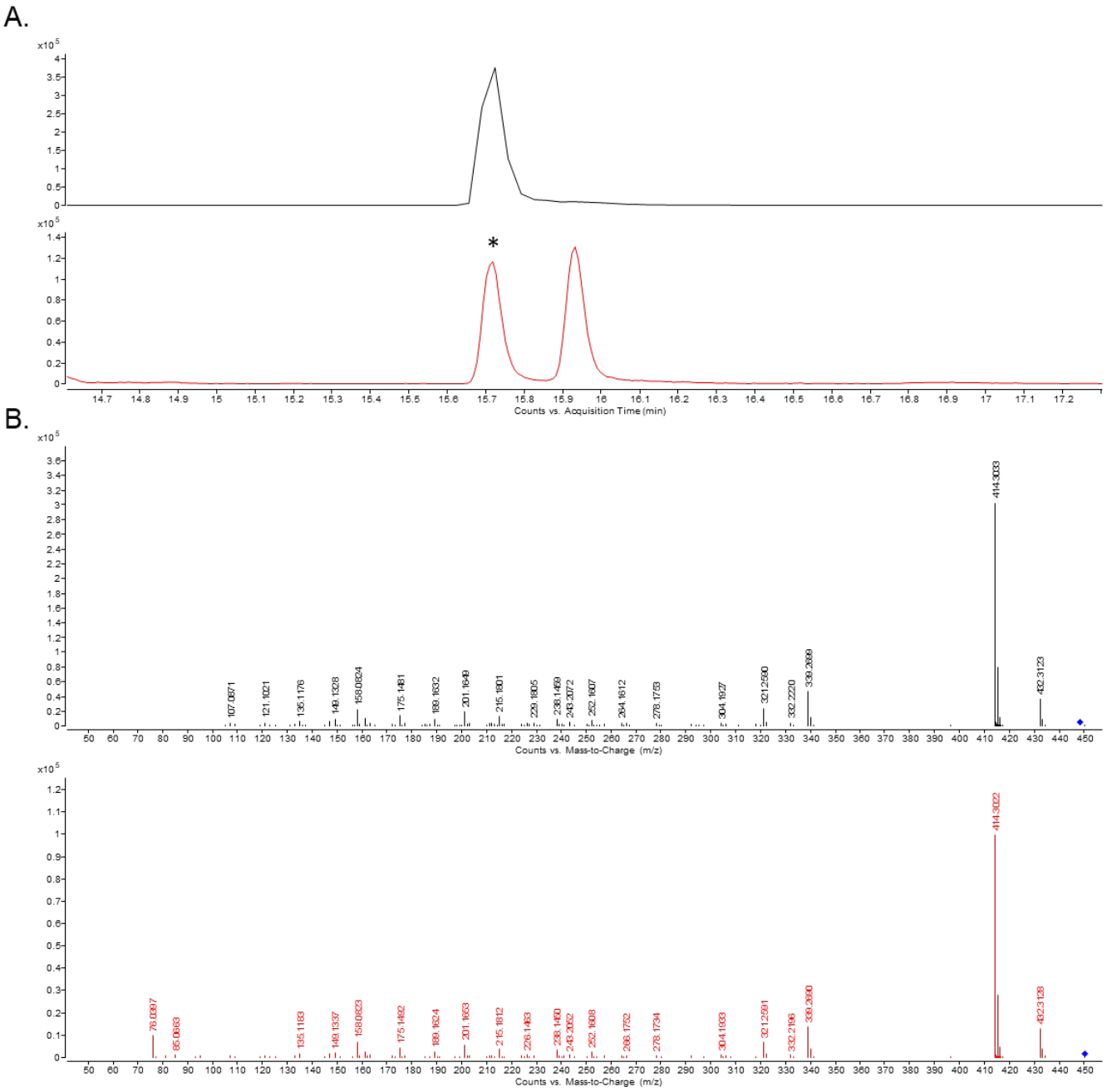

Figure S-17. LC-MS/MS confirmation of glycochenodeoxycholic acid. Extracted ion chromatogram (EIC) for *m/z* 450.3209 (positive mode ionization) demonstrates matching RT in a pooled patient sample and that for glycochenodeoxycholic acid standard (A). MS/MS fragmentation for *m/z* 450.3209 and glycochenodeoxycholic acid resulted in common MS/MS fragmentation patterns (B). Chromatograms and spectra corresponding to the pooled patient sample are depicted in red and those corresponding to the standard are depicted in black. Star indicates the MF peak of interest.

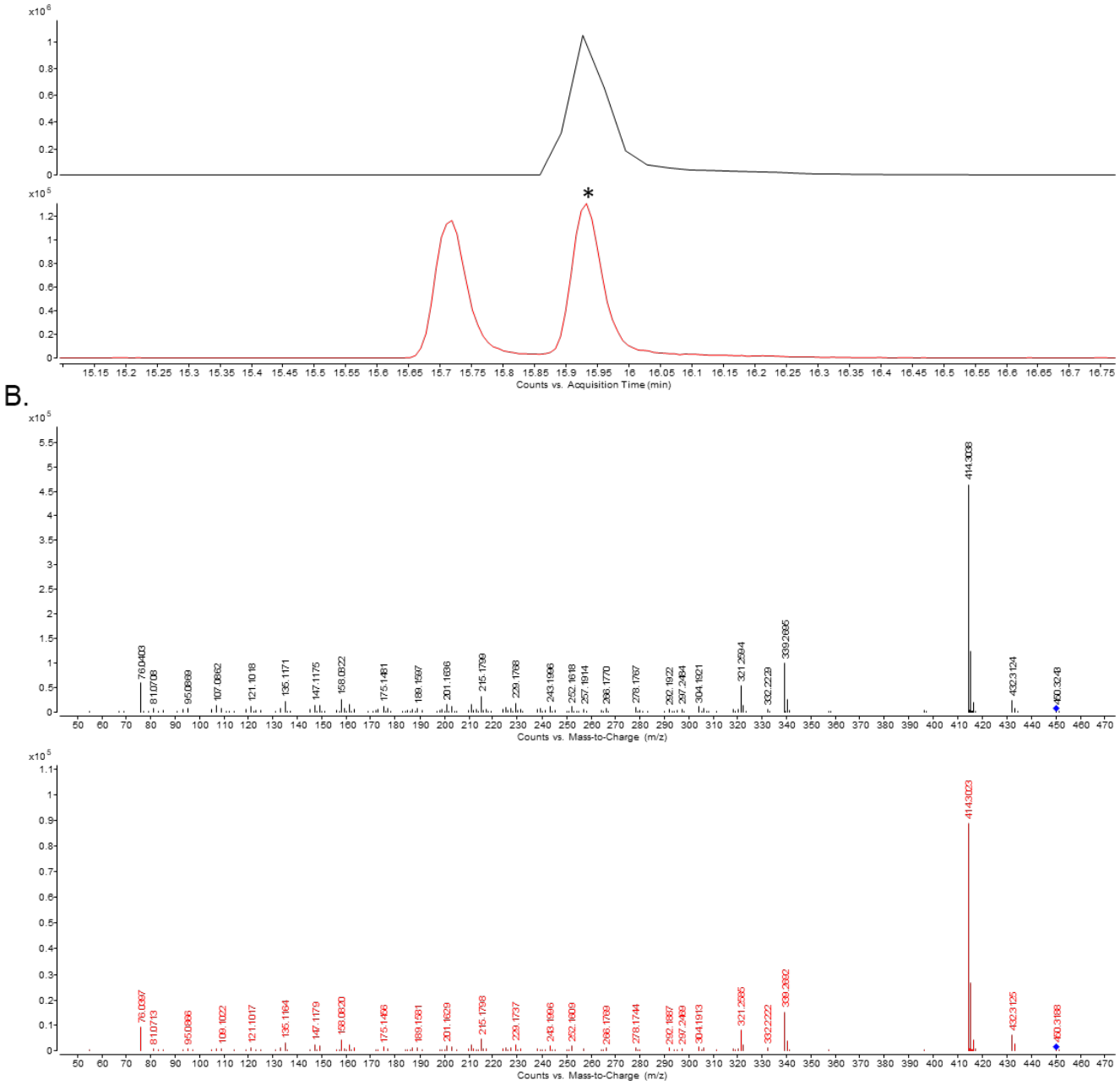

Figure S-18. LC-MS/MS confirmation of MF# 66 as glycodeoxycholic acid. Extracted ion chromatogram (EIC) for *m/z* 450.3209 (positive mode ionization) demonstrates matching RT in a pooled patient sample and that for glycodeoxycholic acid standard (A). MS/MS fragmentation for MF# 66 and glycodeoxycholic acid resulted in common MS/MS fragmentation patterns (B). Chromatograms and spectra corresponding to the pooled patient sample are depicted in red and those corresponding to the standard are depicted in black. Star indicates the MF peak of interest.

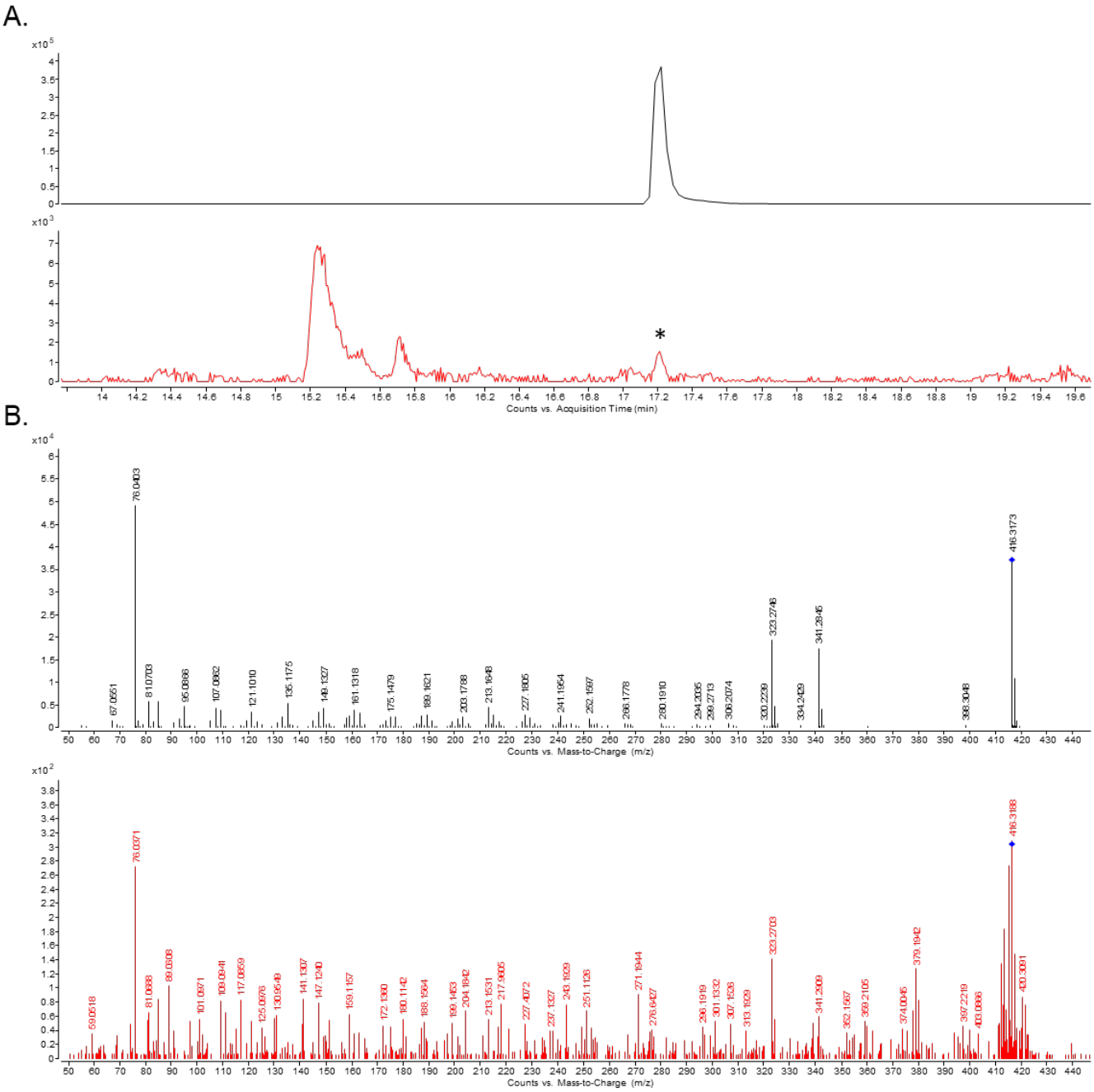

Figure S-19. LC-MS/MS confirmation of MF# 1827 as glycolithocholic acid. Extracted ion chromatogram (EIC) for *m/z* 416.3149 (positive mode ionization) demonstrates matching RT in a pooled patient sample and that for glycolithocholic acid standard (A). MS/MS fragmentation for MF# 1827 and glycolithocholic acid resulted in common MS/MS fragmentation patterns (B). Chromatograms and spectra corresponding to the pooled patient sample are depicted in red and those corresponding to the standard are depicted in black. Star indicates the MF peak of interest.

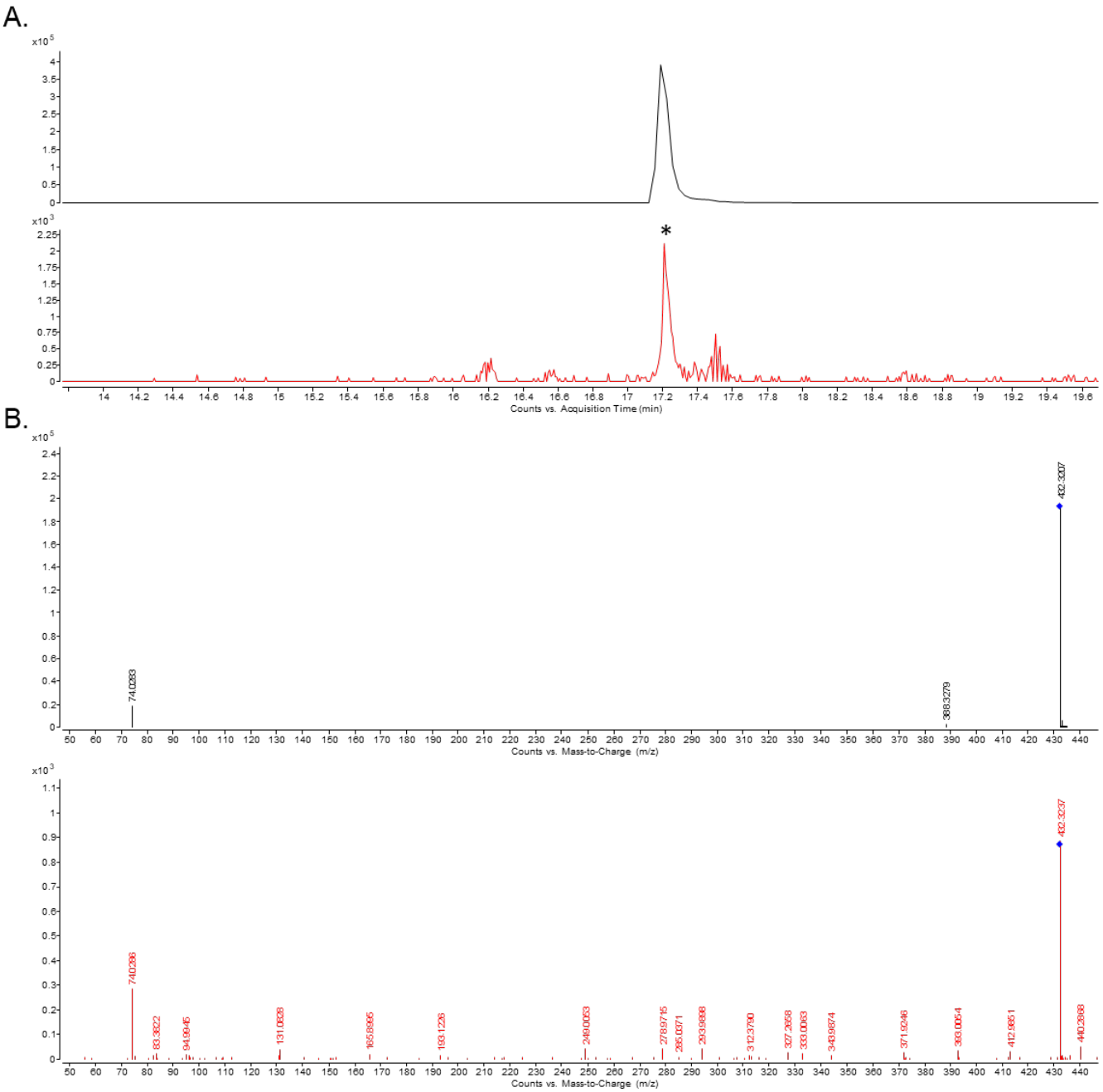

Figure S-20. LC-MS/MS confirmation of MF# 1827 as glycolithocholic acid. Extracted ion chromatogram (EIC) for *m/z* 432.3119 (negative mode ionization) demonstrates matching RT in a pooled patient sample and that for glycolithocholic acid standard (A). MS/MS fragmentation for MF# 1827 and glycolithocholic acid resulted in common MS/MS fragmentation patterns (B). Chromatograms and spectra corresponding to the pooled patient sample are depicted in red and those corresponding to the standard are depicted in black. Star indicates the MF peak of interest.

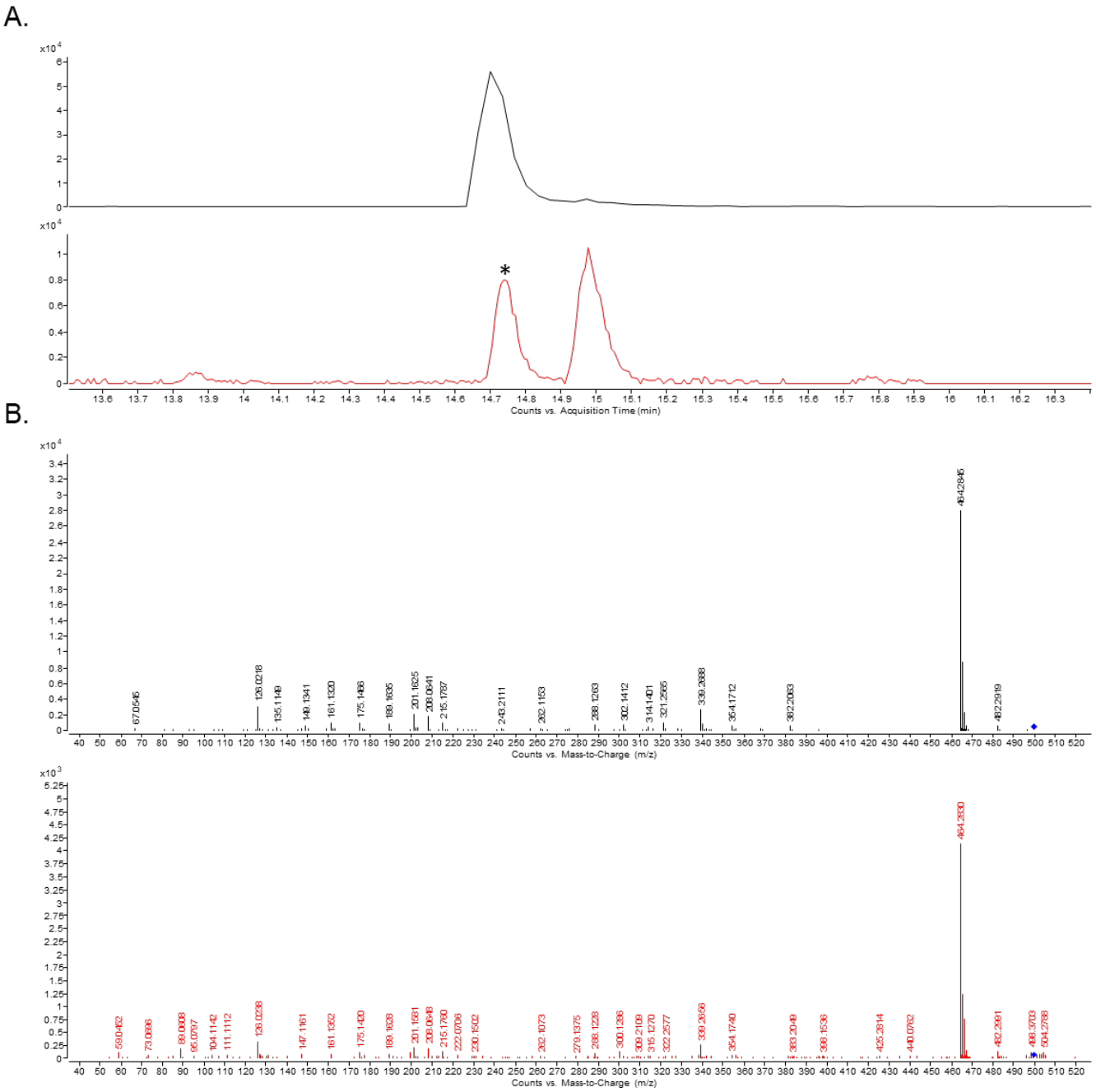

Figure S-21. LC-MS/MS confirmation of taurochenodeoxycholic acid. Extracted ion chromatogram (EIC) for *m/z* 500.3045 (positive mode ionization) demonstrates matching RT in a pooled patient sample and that for taurochenodeoxycholic acid standard (A). MS/MS fragmentation for *m/z* 500.3045 and taurochenodeoxycholic acid resulted in common MS/MS fragmentation patterns (B). Chromatograms and spectra corresponding to the pooled patient sample are depicted in red and those corresponding to the standard are depicted in black. Star indicates the MF peak of interest.

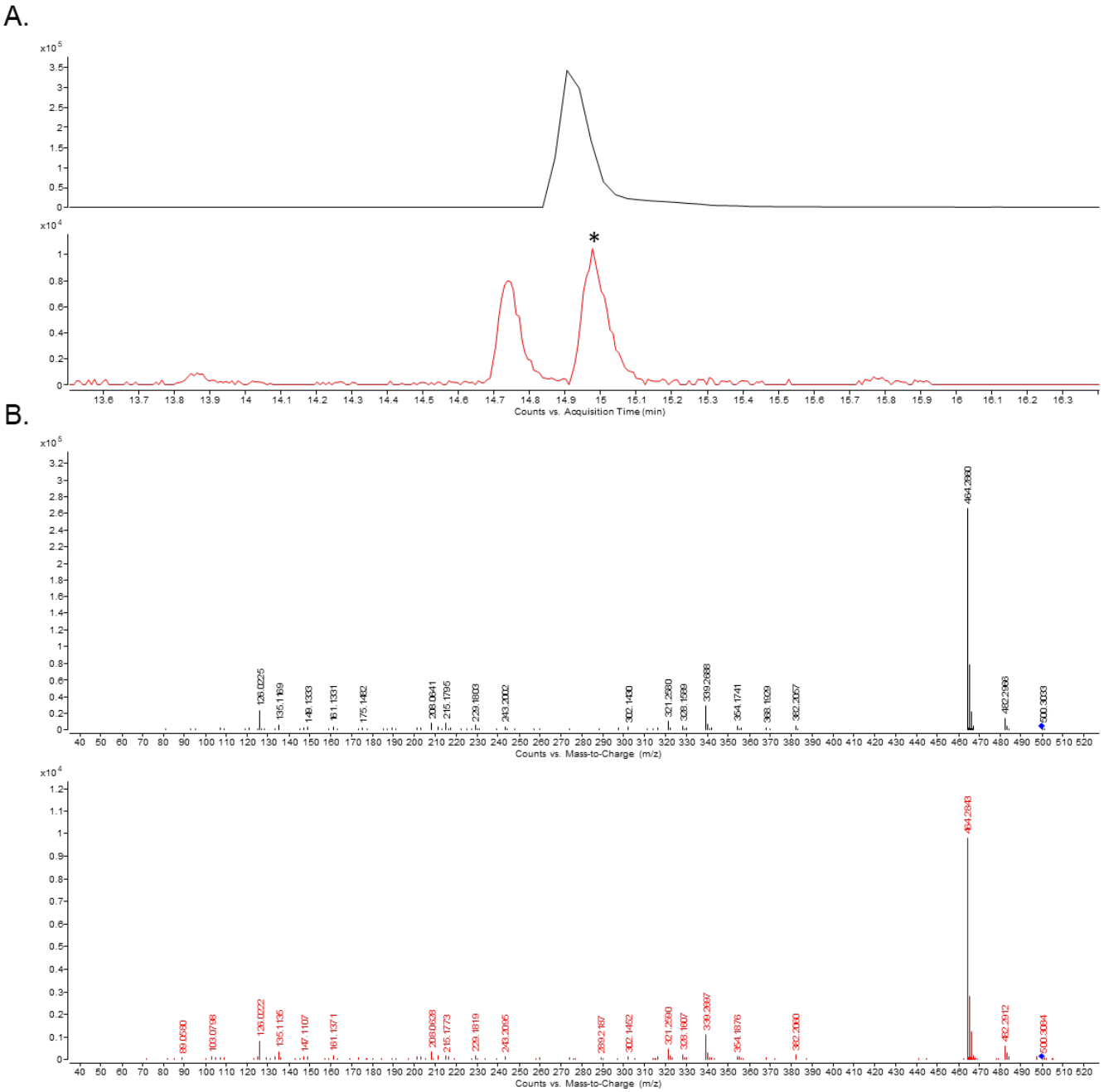

Figure S-22. LC-MS/MS confirmation of MF# 1780 as taurodeoxycholic acid. Extracted ion chromatogram (EIC) for *m/z* 500.3045 (positive mode ionization) demonstrates matching RT in a pooled patient sample and that for taurodeoxycholic acid standard (A). MS/MS fragmentation for MF# 1780 and taurodeoxycholic acid resulted in common MS/MS fragmentation patterns (B). Chromatograms and spectra corresponding to the pooled patient sample are depicted in red and those corresponding to the standard are depicted in black. Star indicates the MF peak of interest.

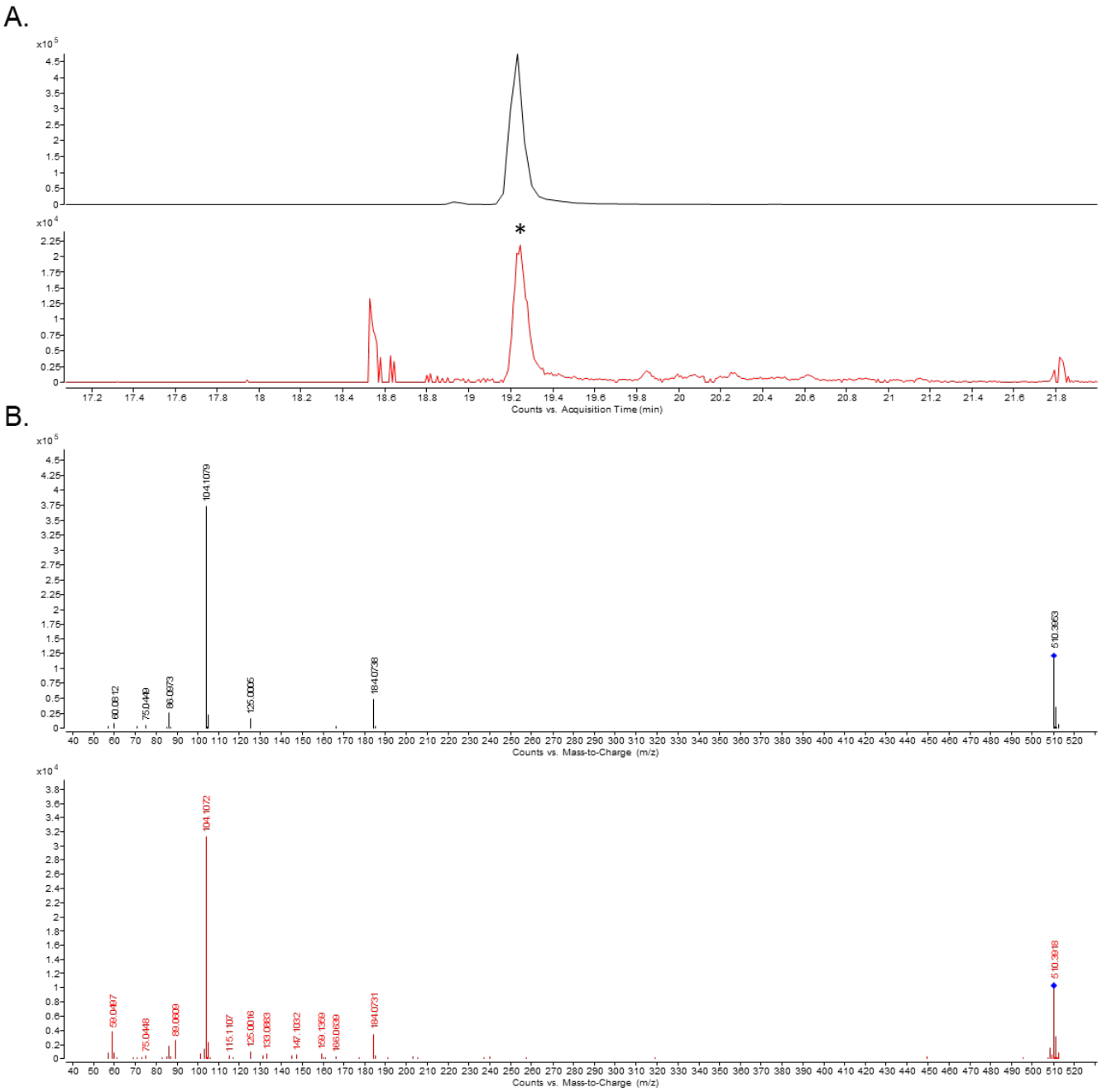

Figure S-23. LC-MS/MS confirmation of MF# 1264 as 1-octadecylglycero-3-phosphocholine (lyso-PAF (C18)). Extracted ion chromatogram (EIC) for *m/z* 510.3924 (positive mode ionization) demonstrates matching RT in a pooled patient sample and that for 1-octadecylglycero-3-phosphocholine standard (A). MS/MS fragmentation for MF# 1264 and 1-octadecylglycero-3-phosphocholine resulted in common MS/MS fragmentation patterns (B). Chromatograms and spectra corresponding to the pooled patient sample are depicted in red and those corresponding to the standard are depicted in black. Star indicates the MF peak of interest.

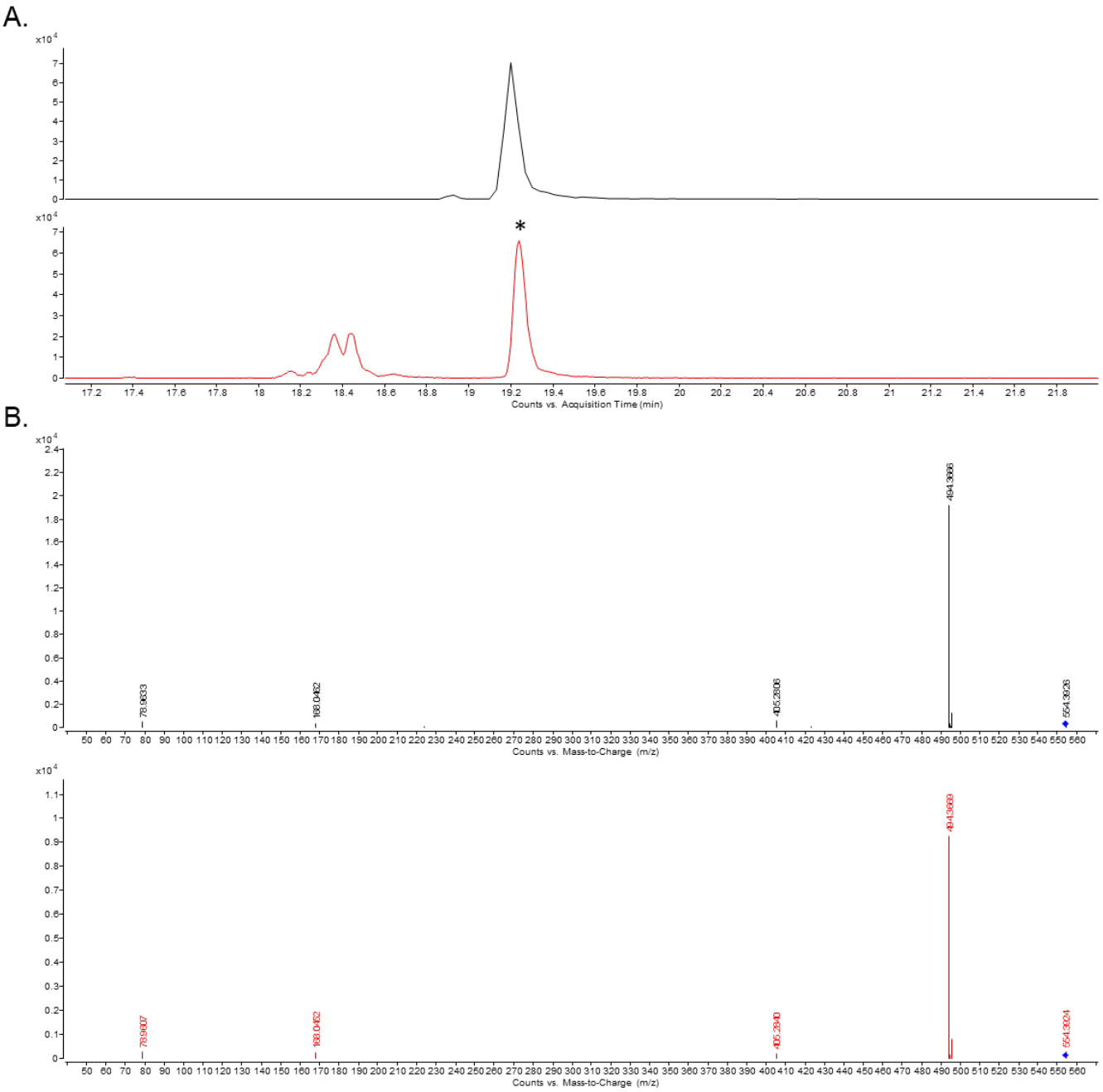

Figure S-24. LC-MS/MS confirmation of MF# 1264 as 1-octadecylglycero-3-phosphocholine (lyso-PAF (C18)). Extracted ion chromatogram (EIC) for *m/z* 554.3839 (negative mode ionization) demonstrates matching RT in a pooled patient sample and that for 1-octadecylglycero-3-phosphocholine standard (A). MS/MS fragmentation for MF# 1264 and 1-octadecylglycero-3-phosphocholine resulted in common MS/MS fragmentation patterns (B). Chromatograms and spectra corresponding to the pooled patient sample are depicted in red and those corresponding to the standard are depicted in black. Star indicates the MF peak of interest.

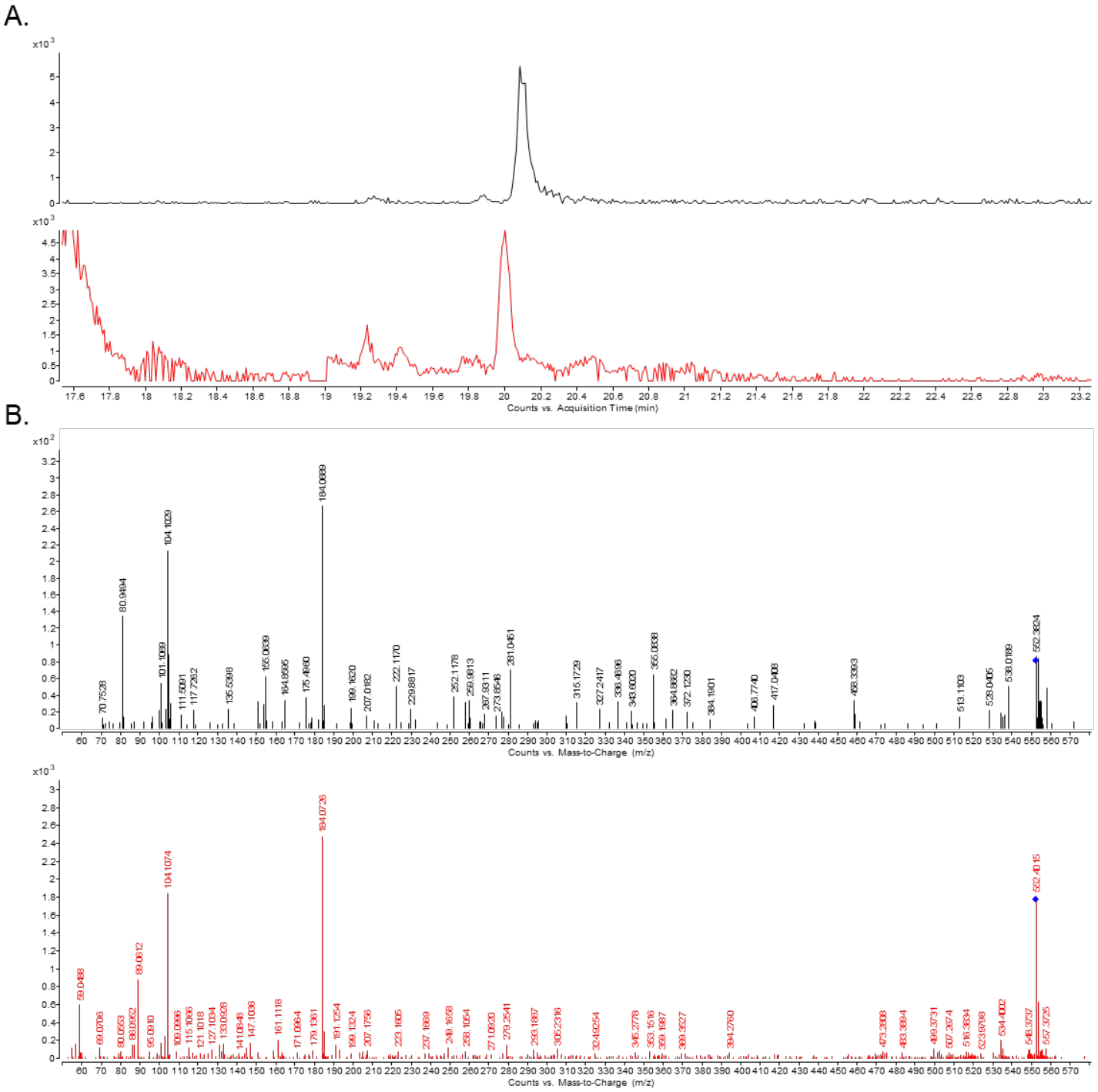

Figure S-25. LC-MS/MS confirmation of MF# 923 as 1-eicosanoyl-sn-glycero-3-phosphocholine (lysoPC (20:0)). Extracted ion chromatogram (EIC) for *m/z* 552.4023 (positive mode ionization) demonstrates matching RT in a pooled patient sample and that for 1-eicosanoyl-sn-glycero-3-phosphocholine standard (A). MS/MS fragmentation for MF# 923 and 1-eicosanoyl-sn-glycero-3-phosphocholine resulted in common MS/MS fragmentation patterns (B). Chromatograms and spectra corresponding to the pooled patient sample are depicted in red and those corresponding to the standard are depicted in black.

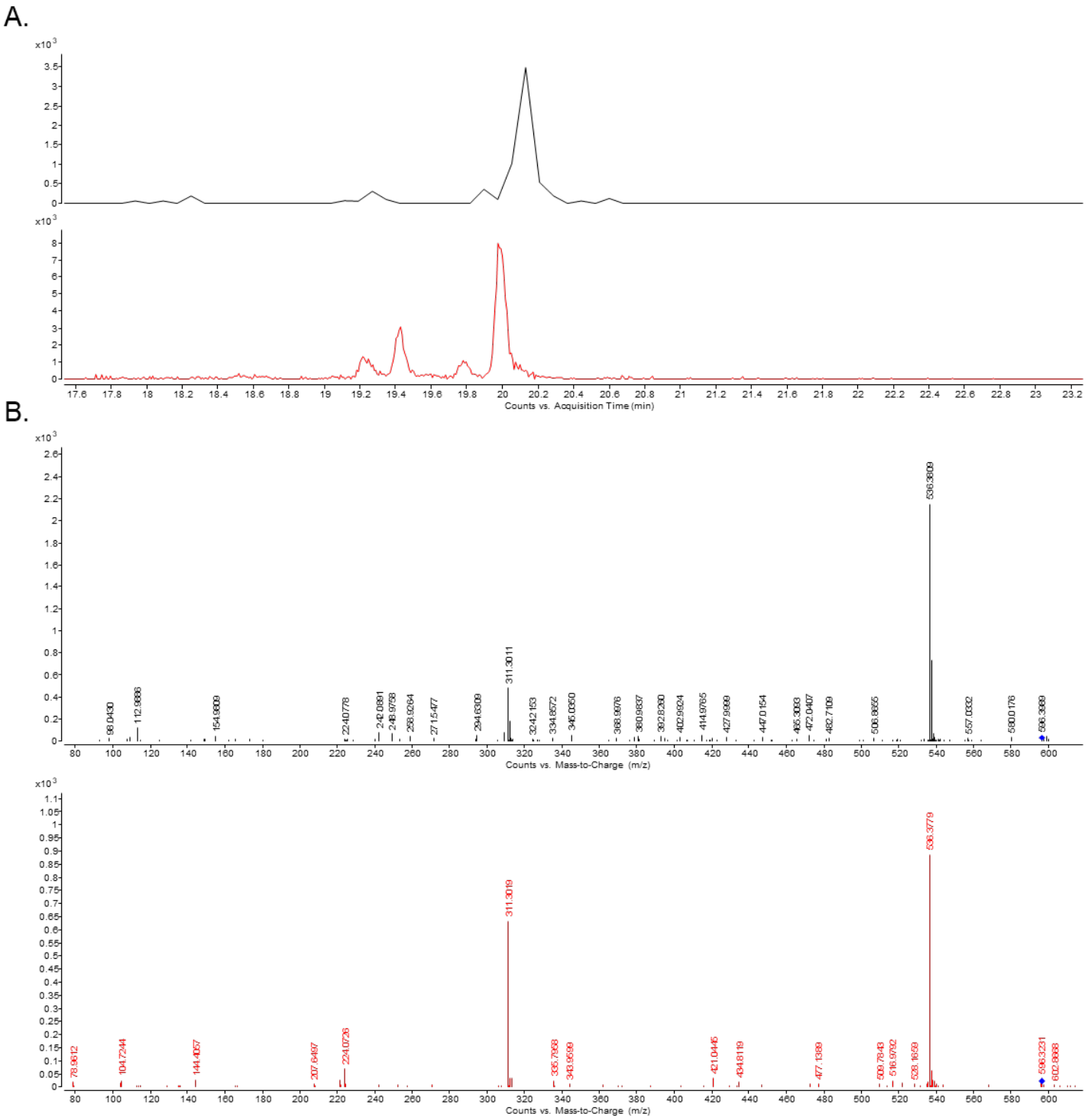

Figure S-26. LC-MS/MS confirmation of MF# 923 as 1-eicosanoyl-sn-glycero-3-phosphocholine (lysoPC (20:0)). Extracted ion chromatogram (EIC) for *m/z* 596.3931 (negative mode ionization) demonstrates matching RT in a pooled patient sample and that for 1-eicosanoyl-sn-glycero-3-phosphocholine (A). MS/MS fragmentation for MF# 923 and 1-eicosanoyl-sn-glycero-3-phosphocholine resulted in common MS/MS fragmentation patterns (B). Chromatograms and spectra corresponding to the pooled patient sample are depicted in red and those corresponding to the standard are depicted in black.

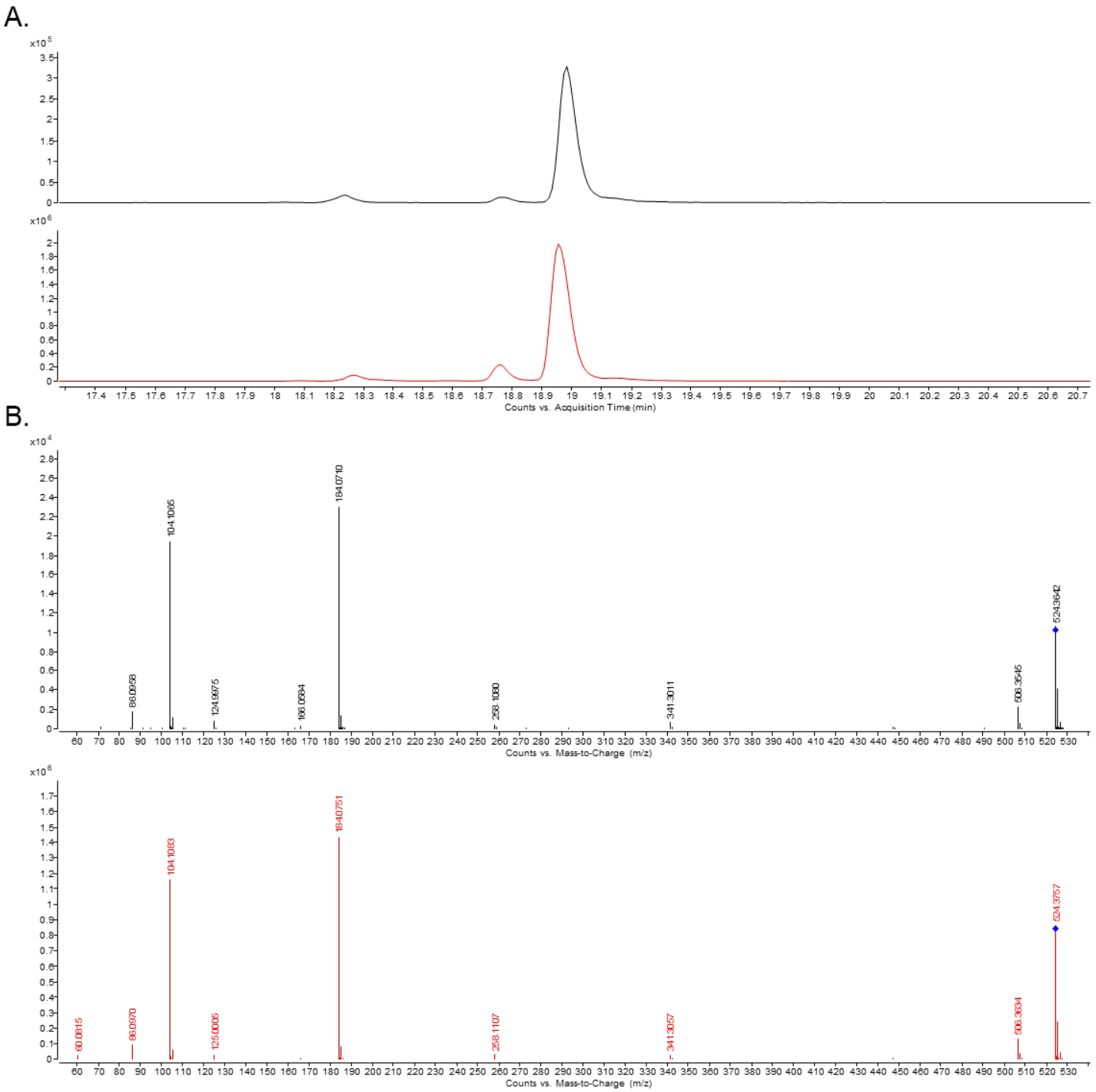

Figure S-27. LC-MS/MS confirmation of MF# 253 as 1-octadecanoyl-sn-glycero-3-phosphocholine (lysoPC (18:0)). Extracted ion chromatogram (EIC) for *m/z* 524.3738 (positive mode ionization) demonstrates matching RT in a pooled patient sample and that for 1-octadecanoyl-sn-glycero-3-phosphocholine standard (A). MS/MS fragmentation for MF# 253 and 1-octadecanoyl-sn-glycero-3-phosphocholine resulted in common MS/MS fragmentation patterns (B). Chromatograms and spectra corresponding to the pooled patient sample are depicted in red and those corresponding to the standard are depicted in black.

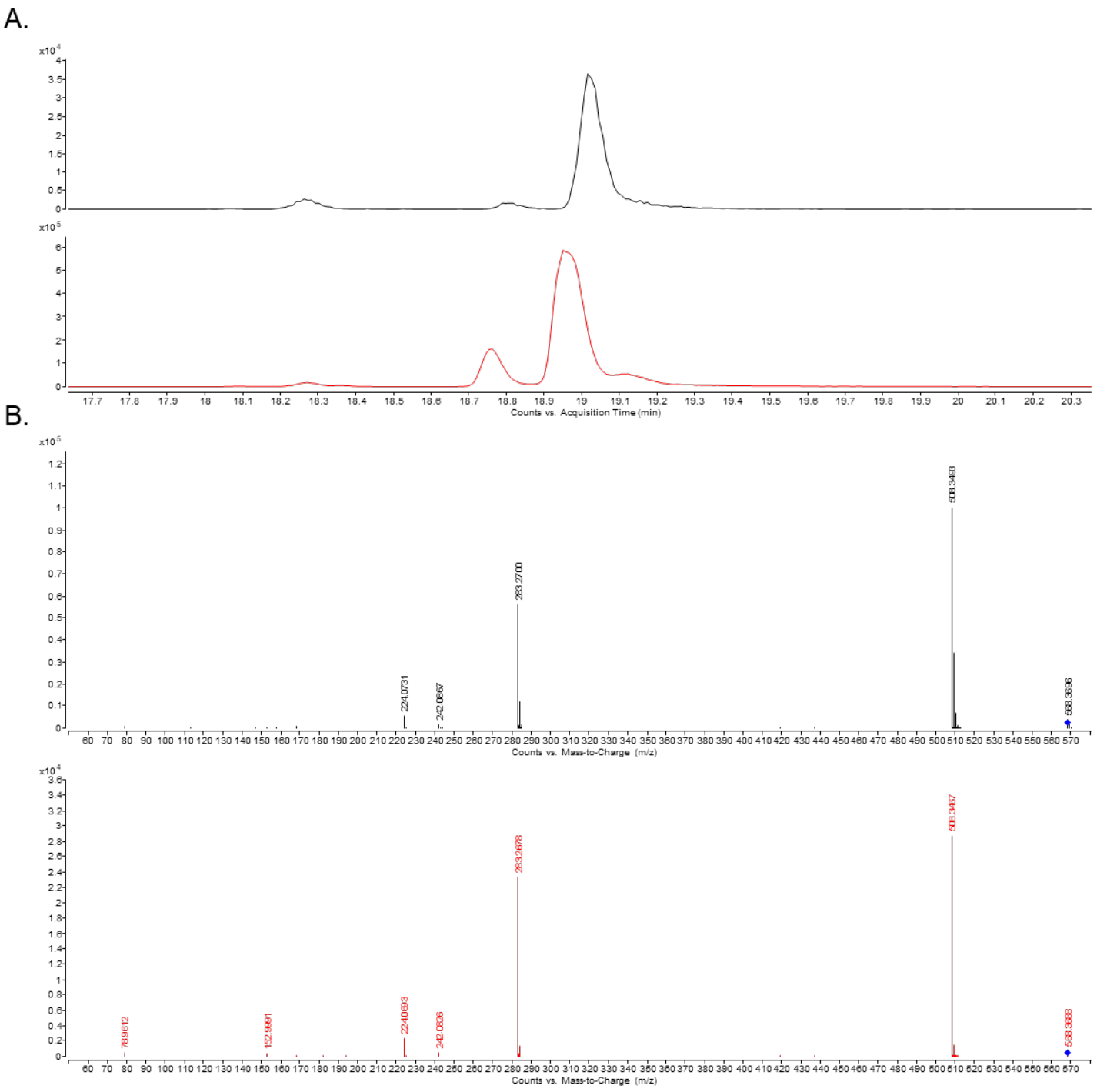

Figure S-28. LC-MS/MS confirmation of MF# 253 as 1-octadecanoyl-sn-glycero-3-phosphocholine (lysoPC (18:0)). Extracted ion chromatogram (EIC) for *m/z* 568.3632 (negative mode ionization) demonstrates matching RT in a pooled patient sample and that for 1-octadecylglycero-3-phosphocholine standard (A). MS/MS fragmentation for MF# 253 and 1-octadecanoyl-sn-glycero-3-phosphocholine resulted in common MS/MS fragmentation patterns (B). Chromatograms and spectra corresponding to the pooled patient sample are depicted in red and those corresponding to the standard are depicted in black.

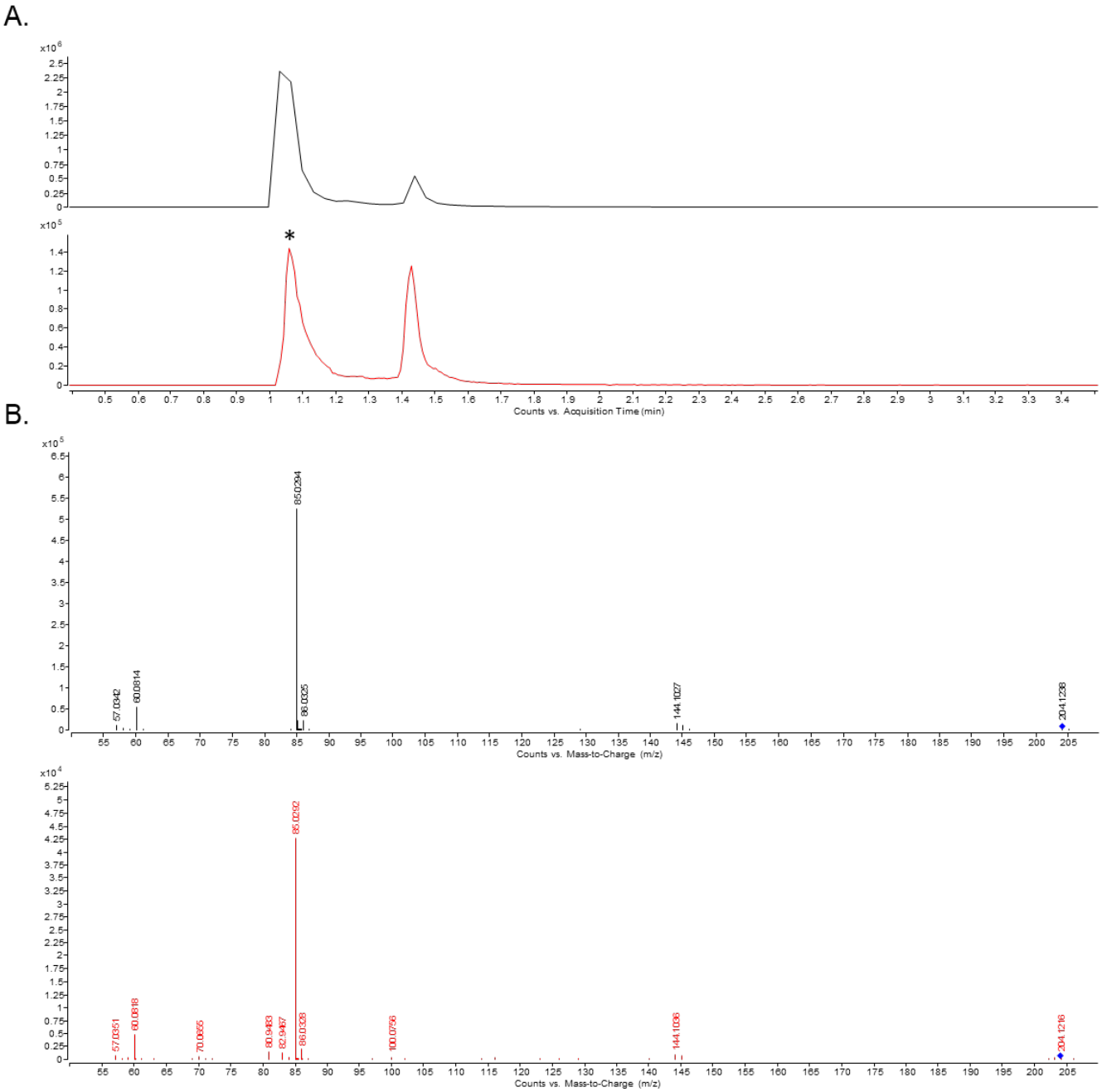

Figure S-29. LC-MS/MS confirmation of MF# 1460 as acetylcarnitine. Extracted ion chromatogram (EIC) for *m/z* 204.1201 (positive mode ionization) demonstrates matching RT in a pooled patient sample and that for acetylcarnitine standard (A). MS/MS fragmentation for MF# 1460 and acetylcarnitine resulted in common MS/MS fragmentation patterns (B). Chromatograms and spectra corresponding to the pooled patient sample are depicted in red and those corresponding to the standard are depicted in black. Star indicates the MF peak of interest.

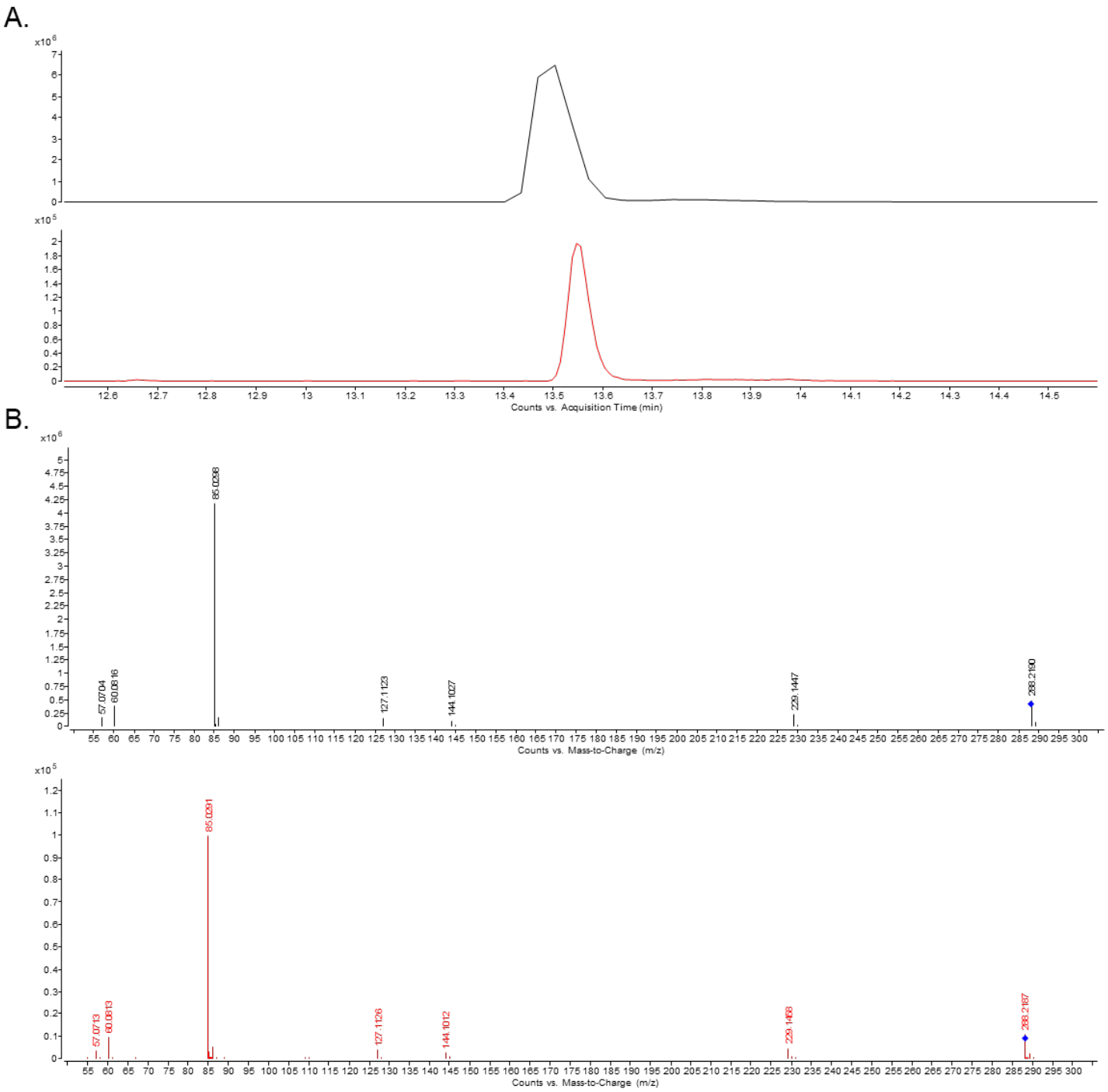

Figure S-30. LC-MS/MS confirmation of MF# 996 as octanoylcarnitine. Extracted ion chromatogram (EIC) for *m/z* 288.2172 (positive mode ionization) demonstrates matching RT in a pooled patient sample and that for octanoylcarnitine standard (A). MS/MS fragmentation for MF# 996 and octanoylcarnitine resulted in common MS/MS fragmentation patterns (B). Chromatograms and spectra corresponding to the pooled patient sample are depicted in red and those corresponding to the standard are depicted in black.

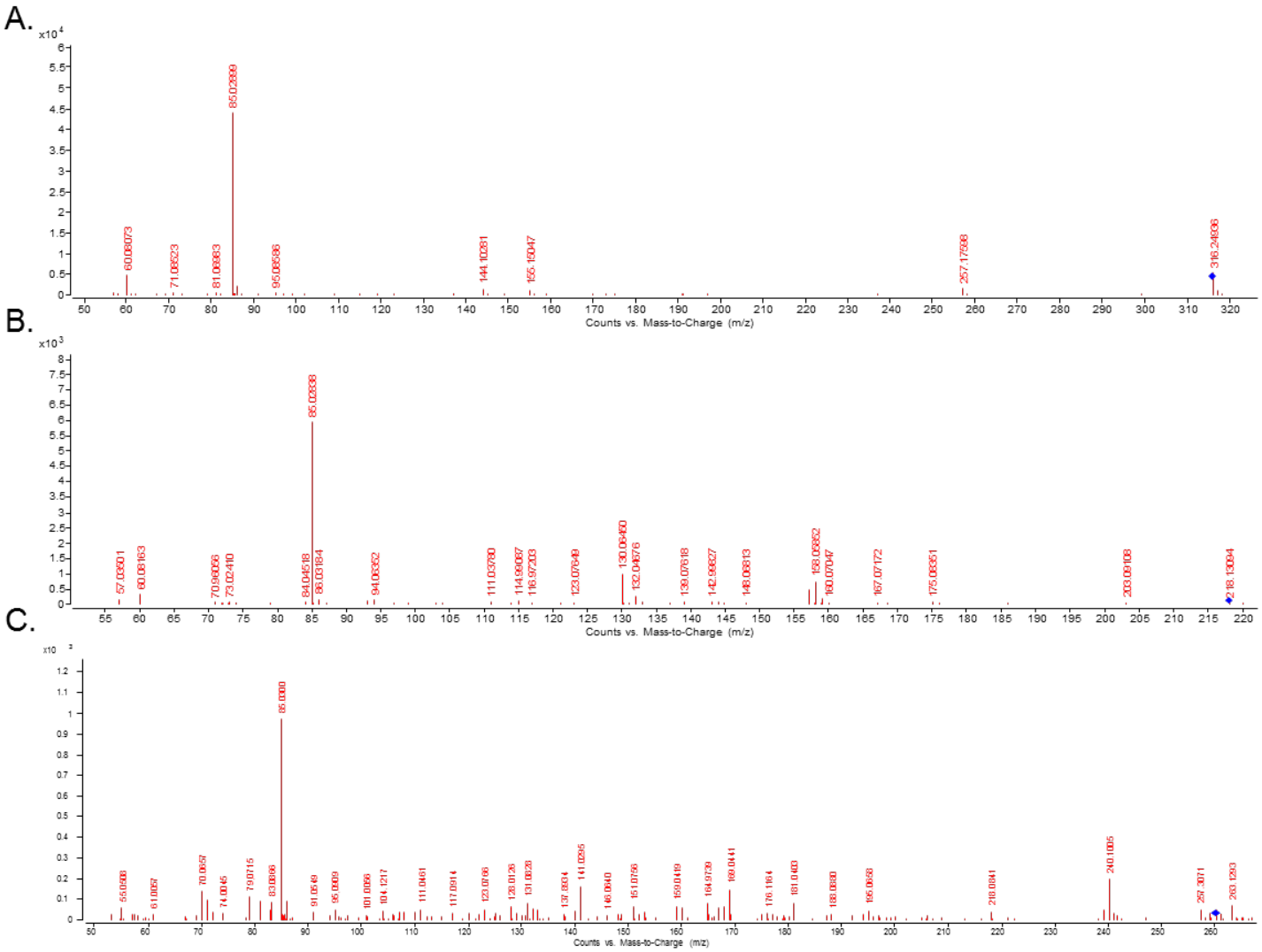

Figure S-31. LC-MS/MS confirmation of decanoylcarnitine. MS/MS fragmentation for *m/z* 316.2491 (positive mode ionization) demonstrates diagnostic fragment ion (*m/z* 85.02899) (A). LC-MS/MS confirmation of propionylcarnitine in positive mode. MS/MS fragmentation for *m/z* 218.1369 demonstrates diagnostic fragment ion (*m/z* 85.02838) (B). LC-MS/MS confirmation of hexanoylcarnitine in positive mode. MS/MS fragmentation for *m/z* 260.1854 demonstrates diagnostic fragment ion (*m/z* 85.0300) (C).

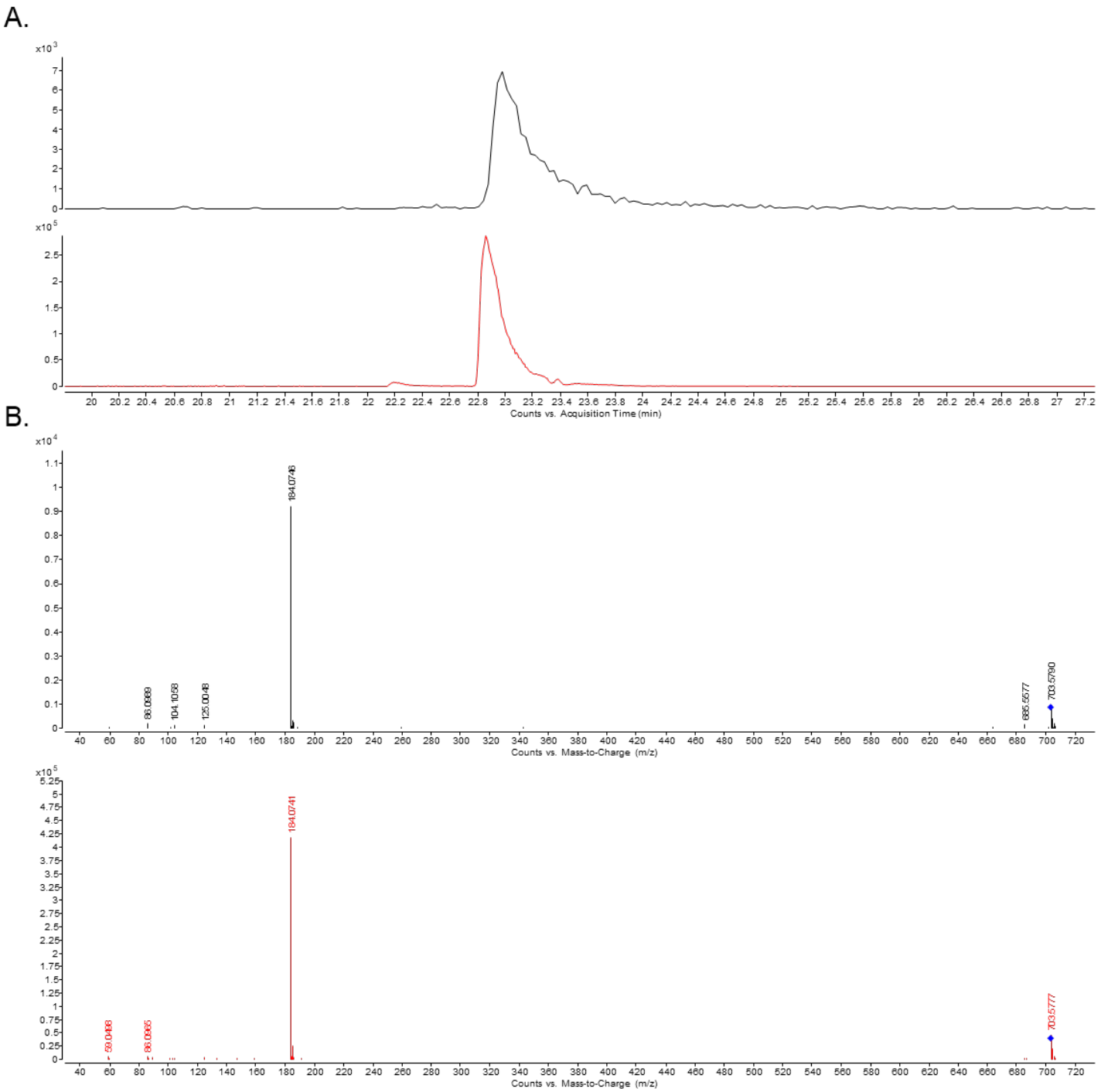

Figure S-32. LC-MS/MS confirmation of MF# 134 as sphingomyelin (d18:1/16:0). Extracted ion chromatogram (EIC) for *m/z* 703.5742 (positive mode ionization) demonstrates matching RT in a pooled patient sample and that for sphingomyelin (d18:1/16:0) standard (A). MS/MS fragmentation for MF# 134 and sphingomyelin (d18:1/16:0) resulted in common MS/MS fragmentation patterns (B). Chromatograms and spectra corresponding to the pooled patient sample are depicted in red and those corresponding to the standard are depicted in black.

A.

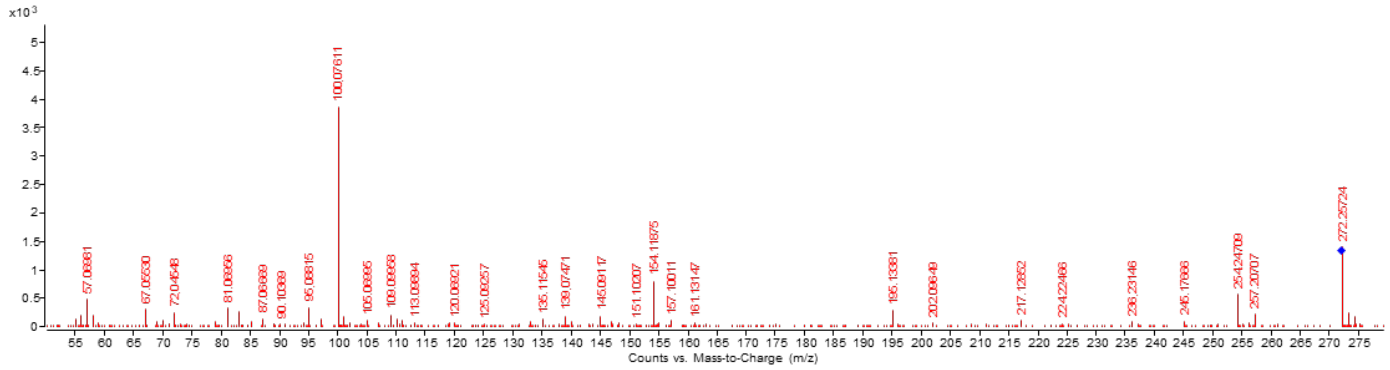

Figure S-33. LC-MS/MS confirmation of MF# 189 as sphingosine (d16:1). MS/MS fragmentation for MF# 189 (*m/z* 272.2583, positive mode ionization) resulted in diagnostic MS/MS fragment ions *m/z* 254.4709, *m/z* 236.2315, and *m/z* 224.2247 corresponding to $[M+H - H_2O]^+$, $[M+H - 2H_2O]^+$, and $[M+H - H_2O - CH_2O]^+$, respectively (A).

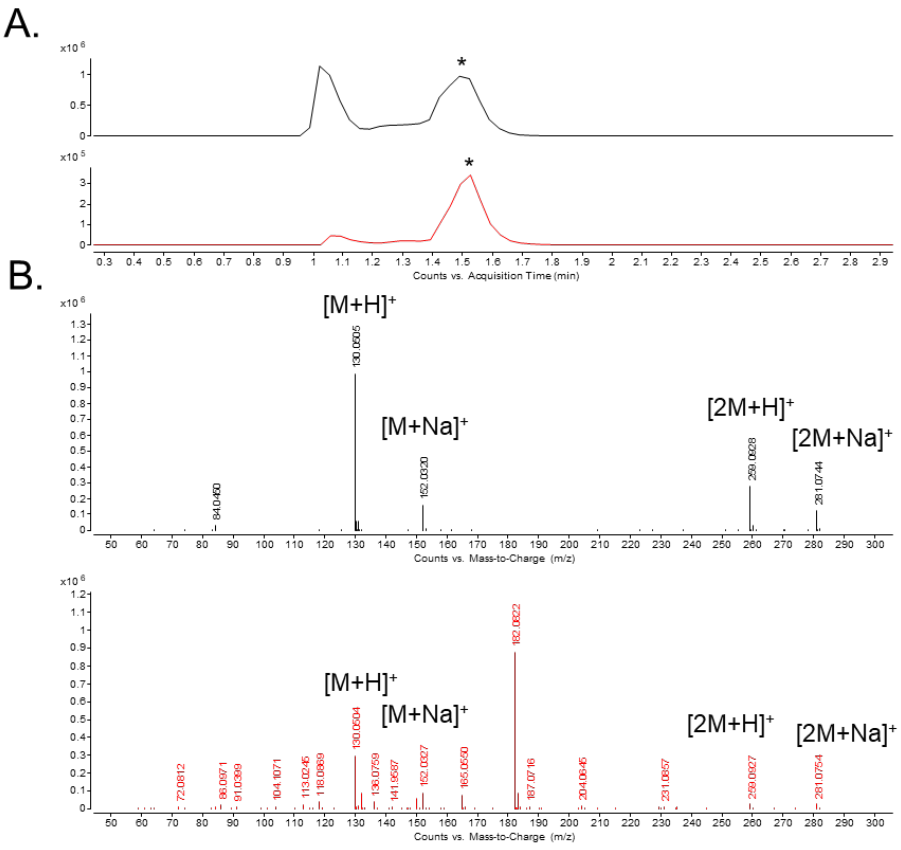

Figure S-34. LC-MS confirmation of MF# 2 as 5-oxo-proline. Extracted ion chromatogram (EIC) for *m/z* 130.0499 (positive mode ionization) demonstrates matching RT in a pooled patient sample and that for 5-oxo-proline standard (A). MS for MF# 2 resulted in common MS adducts between 5-oxo-proline standard and pooled sample corresponding to $[M+H]^+$, $[M+Na]^+$, $[2M+H]^+$, and $[2M+Na]^+$ (B). Chromatograms and spectra corresponding to the pooled patient sample are depicted in red and those corresponding to the standard are depicted in black.